Co-targeting CDK 4/6 and C-MYC/STAT3/CCND1 axis and inhibition of tumorigenesis and epithelial-mesenchymal-transition in triple negative breast cancer by Pt(II) complexes bearing NH3 as trans-co-ligand

Zhimin Lv, Amjad Ali, Na Wang, Haojie Ren, Lijing Liu, Fufu Yan, Man Shad, Huifang Hao, Yongmin Zhang, Faiz-Ur Rahman

Co-targeting CDK 4/6 and C-MYC/STAT3/CCND1 axis and inhibition of tumorigenesis and epithelial-mesenchymal-transition in triple negative breast cancer by Pt(II) complexes bearing NH_3 as *trans*-co-ligand

Zhimin Lv[a,#], Amjad Ali[b,c,#], Na Wang[a], Haojie Ren[a], Lijing Liu[a], Fufu Yan[a], Man Shad[a,d], Huifang Hao[a,d], Yongmin Zhang[a,e,*] and Faiz-Ur Rahman[a,*]

[a]Inner Mongolia University Research Center for Glycochemistry of Characteristic Medicinal Resources, Department of Chemistry and Chemical Engineering, Inner Mongolia University, Hohhot People's Republic of China

[b]Institute of Integrative Biosciences, CECOS University of IT and Emerging Sciences, Peshawar, KPK, Pakistan.

[c]Institute of Biomedical Sciences, School of Life Sciences, East China Normal University, 500 Dongchuan Road, Shanghai, 200241, People's Republic of China.

[d]School of Life Sciences, Inner Mongolia University, Hohhot 010021, People's Republic of China.

[e]Sorbonne Université, CNRS, Institut Parisien de Chimie Moléculaire, UMR 8232, 4 Place Jussieu, 75005 Paris, France.

# These authors contributed equally to this work.

*Corresponding Authors E-mail: Yongmin.zhang@upmc.fr (Y. Zhang), faiz@imu.edu.cn (F.-U. Rahman)

Abstract

In search of potential anticancer agents, we synthesized SNO-donor salicylaldimine main ligand-based Pt(II) complexes bearing NH_3 as co-ligand at *trans*-position (**C1-C6)**. These complexes showed similarity in structure with transplatin as the two N donor atoms of the main ligand and NH_3 co-ligand were coordinated to Pt in *trans* position to each other. Each complex with different substituents on the main ligand was characterized thoroughly by detailed spectroscopic and spectrophotometric methods. Four of these complexes were studied in solid state by single crystal X-ray analysis. The stability of reference complex **C1** was measured in solution state in DMSO-d_6 or its mixture with D_2O using ^{1}H NMR methods.

These complexes were further investigated for their anticancer activity in triple-negative-breast (TNBC) cells including MDA-MB-231, MDA-MB-468 and MDA-MB-436 cells. All these complexes showed satisfactory cytotoxic effect as revealed by the MTT results. Importantly, the highly active complex **C4** anticancer effect was compared to the standard chemotherapeutic agents including cisplatin, oxaliplatin and 5-fluorouracil (5-FU). Functionally, **C4** suppressed invasion, spheroids formation ability and clonogenic potential of cancer cells. **C4** showed synergistic anticancer effect when used in combination with palbociclib, JQ1 and paclitaxel in TNBC cells. Mechanistically, **C4** inhibited cyclin-dependent kinase (CDK)4/6 pathway and targeted the expressions of MYC/STAT3/CCND1/CNNE1 axis. Furthermore, **C4** suppressed the EMT signaling pathway that suggested a role of **C4** in the inhibition of TNBC metastasis. Our findings may pave further in detailed mechanistic study on these complexes as potential chemotherapeutic agents in different types of human cancers.

Keywords

Ammonia ligand, TNBC, metastasis, tumor spheroids, CDK4/6, EMT expression

Introduction

Triple-negative breast cancer (TNBC) is the most aggressive molecular subtype of breast cancer associated with higher metastasis, relapse and mortality rates. TNBC is a heterogeneous disease that arises due to several genetic and epigenetic changes [1]. TNBC patients show metastasis to lungs, liver and other parts of the body. Survival rates of TNBC are less than five years and most of the TNBC patients show poor prognosis and diagnosis [2]. Epithelial-mesenchymal-transition, invasion, migration, increased cell cycle progression and abnormal growth are the common features of TNBC cells [3]. TNBC patients show resistance to chemotherapy due to the aggressiveness of this disease. Oncogenic signaling pathways play key roles in the development, progression, metastasis and chemoresistance of TNBC [4]. Blocking or inhibition of oncogenic signaling pathways in TNBC with novel inhibitors, drugs and anticancer agents are considered important therapeutic approaches for better treatment options [5].

Cyclin-dependent kinase 4/6 (CDK4/6) plays an important role in cell cycle progression by increasing DNA synthesis. CDK4/6 has been shown to promote invasion, migration, tumorigenesis and play key roles in metastasis [6]. Inhibition of CDK4/6 is associated with increased apoptosis and decreased cell survival, invasion and metastasis [7]. Deregulation or abnormal regulation of CDK4/6 leads to uncontrolled and sustained cell growth. CDK4/6 pathway is highly activated in different molecular subtypes of breast cancers including TNBC and mainly targets the G1/S transition. CKD4 knockout has been shown to prevent breast cancer development [8]. CDK4/6 pathway form a complex with cyclinD1

(CDK4/6-cyclinD1 axis) that plays a major role in the development, tumorigenesis and metastasis of breast cancer. CDK4/6 pathway is linked with important signaling proteins including RB, E2F family and cyclin-dependent kinases [9]. Recently several important inhibitors have been identified to block the CDK4/6-cyclinD1 axis and G1/S cyclin-dependent kinases [10]. Therefore, targeting CDK4/6 pathway is considered among important therapeutic targets for better treatment of breast cancer patients**.**

Since the approval of cisplatin in 1978, platinum drugs have attracted much attention in the field of oncology. Subsequently, carboplatin and oxaliplatin were approved for marketing in 1989 and 2002, respectively. These three drugs have been widely used worldwide. During this period, some other platinum drugs have also been approved on a small scale in specific country, such as nedaplatin, heptaplatin, lobaplatin, miriplatin and bicycloplatin (Fig. 1) [11]. Taking cisplatin as an example, after the drug enters the cancer cell it is hydrated, the "Cl" ancillary ligand attached to platinum (II) is replaced by H_2O molecule through ligand exchange to form the activated pt(II) drug [12-13]. Only a small number of active species can enter the nucleus and effectively bind to the N7 position of the most nucleophilic guanine base in DNA [14-16]. Platinum inter-/intra-strand crosslinks to double strand helical DNA minor groove forms metal-DNA adduct that distorts the structure of DNA molecule, inhibits DNA transcription and replication, and ultimately leads to apoptosis [17-20].

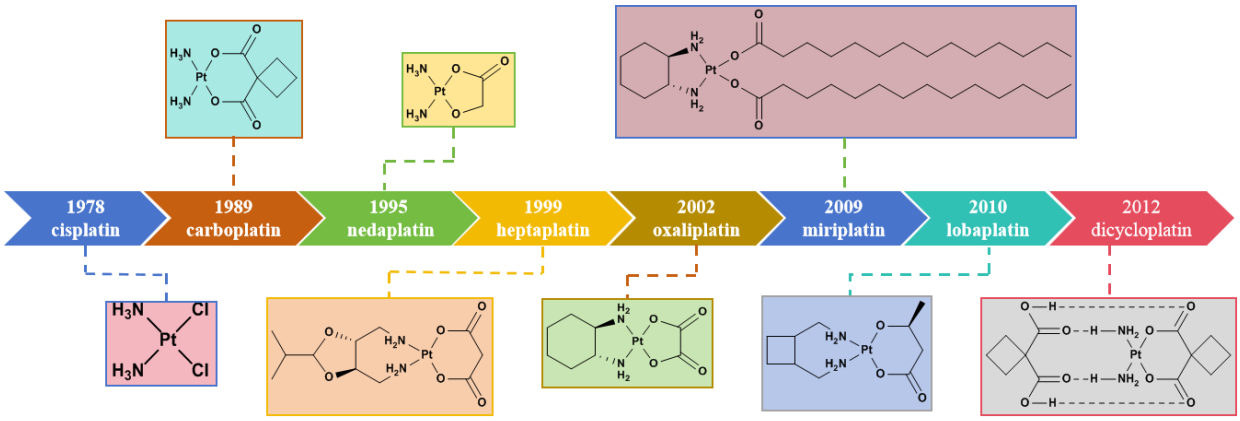

Fig. 1. Clinically administered (approved) anticancer drugs of platinum, the year it is approved

With the wide application of platinum drugs, chemotherapy resistance, increased incidence of side effects and economic costs could not be ignored, which limits the application of platinum drugs [21-23]. Based on these shortcomings of the presently approved platinum-based drugs, a lot of research has been carried out in the recent years to overcome these limitations. These novel platinum anticancer drugs reported were mainly presented with ligand modification, biomolecular assembly, binding with other clinically approved drugs, delivery vehicles etc. [24-30]. Similarly, the use of these different coordination

assemblies in these newly developed platinum anticancer complexes changed the targets inside cancer cells [31-37]. Several new platinum complexes reported with good anticancer properties are under clinical trials therefore, the development of new platinum complexes is still important for the development of future anticancer drugs [38-42]. Platinum drugs represent a unique class of DNA damaging agents, in the past few decades, cisplatin has been used an active antitumor drug, but the development of adverse reactions and drug resistance has limited the use of cisplatin [43]. Compared with cisplatin, transplatin is inactive *in vivo* and has low cytotoxicity *in vitro*, but its derivatives have significant *in vitro* antitumor activity against a variety of tumor cells (including cisplatin-resistant cells) [44-45]. The first report on biologically active transplatin derivatives was the replacement of NH_3 ligand(s) with planar amines such as pyridine to get an active complex with cytotoxicity equivalent to cisplatin [46]. After that, some planar N-heterocycles (pyridine, isoquinoline, quinoline, thiazole etc.) were introduced as ligands to study the anticancer activity [47-50]. N-heterocyclic carbene (NHC) ligands are easy to obtain, structurally modified and reported to be tightly bind to metals, has been widely used ligands in bioinorganic metal-based drugs or transplatin derivatives [51-57]. Since the hydrophobic ligand modification of some transplatin derivatives showed better antitumor activity in some cancer cell lines therefore, these ligands such as PPh_3 were also used in the synthesis of biologically active derivatives [58]. Hydrazone ligands have attracted much attention due to their multifunctional coordination ability and potential applications in medicine and biology. They are also widely used in the synthesis of platinum complexes used in anticancer studies [59-61]. Ana I. Matesanz et al. reported platinum complexes based on N-*p*-chlorophenyl thiosemicarbazone as ligands for their pharmacological properties, these complexes were reported to show high selectivity for tumor cells and lack of activity in healthy cells [62]. These recent studies carried out in the field of platinum based anticancer drugs area encourage us and many other researchers to design and synthesize novel Pt-based anticancer complexes with novel organic assemblies.

In our previous studies we synthesized salicylaldimine type Schiff base ligands bearing ON, ONS, ONN coordinating atoms and used them in the synthesis of Pt/Ru complexes with good anticancer activities [63-64]. In the current study we synthesized a series of Pt(II) complexes bearing a ONS-donor tri-coordinated Schiff base as a major ligand and N-donor NH_3 as a co-ligand coordinated at *trans* position to the N donor atom of the main ligand and studied their anticancer effects in triple negative breast cancer cells (TNBC). The structures and stabilities of these complexes were determined in detail by ^{1}H, ^{13}C NMR, UV-vis, FT-IR spectroscopy and HR-ESI mass spectrometry. The solid-state single crystal X-ray analysis was used to confirm the exact coordination of the ligands and Pt center. We examined their ability to inhibit cell growth and colony formation in different TNBC cell lines (MDA-MB-231, MDA-MB-468 and MDA-MB-436 cells) and analyzed the effects of the highly active complex on tumor stem

cell formation, cell migration and cell senescence. Similarly, cancer cell invasion, stemness and EMT of TNBC by targeting the C-MYC/STAT3/CCND1/CNNE1 and p27 axis by down-regulating cyclin-dependent kinase (CDK)4/6 studies were also conducted.

2. Results

2.1. Chemistry

*2.1.1. Synthesis and characterization of **C1-C6***

Starting complexes **SC1-SC6** [63, 65] were used to synthesize **C1-C6**. Starting complex (**SC1-SC6**) was taken in 40% MeOH/DCM and added with slight excess of solid $AgBF_4$ and stirred for 12 h at reflux. After disappearance of the reactant spot (checked by TLC) the solution was filtered through a pad of celite and the filtrate was added with excess NH_4OH to obtain **C1-C6** (scheme 1). The structure of each complex was characterized by different analytical methods. The difference between **C1-C6** and **SC1-SC6** was clearly observed in the ^1H NMR spectrum. For **C1-C6**, the most obvious proton signal was observed for the co-ligand (NH_3) protons appears in the 5.04-4.97 ppm region [76]. In ^{13}C NMR, the signal of each carbon from the similar structure of **SC1-SC6** moved slightly in **C1-C6** within a reasonable range (Fig. S1-S12). In HR-ESI MS analysis $[M-BF_4]^+$ peak was observed as a major *m/z* for each complex (**C1-C6**) showing the loss of BF_4 anion from each molecule (Fig. S13-S18).

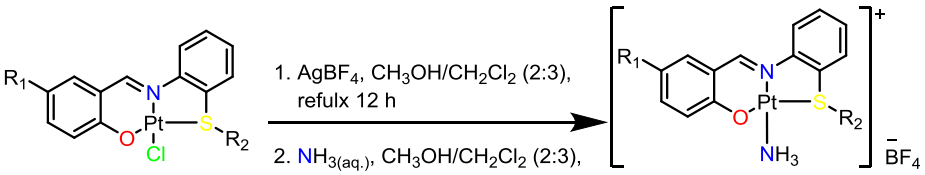

Scheme 1. Synthetic scheme for **C1-C6**

*2.1.2. UV-vis spectroscopic study of **C1-C6***

The UV-vis absorption spectra of **C1-C6** were measured in chloroform solution at room temperature (Fig. 2). The UV-vis absorption spectra of **C1-C6** showed similarity, the obvious absorption peaks near 250 and 330 nm was assigned to the ligand-to-ligand charge transfer (LLCT). Similarly, the metal-to-ligand

charge transfer (MLCT) transition was observed near 460 nm region for **C1-C5** and near 480 nm for **C6**, the slight red shift in absorption peak for **C6** should be due to the presence of electron donor methoxy group on main ligand.

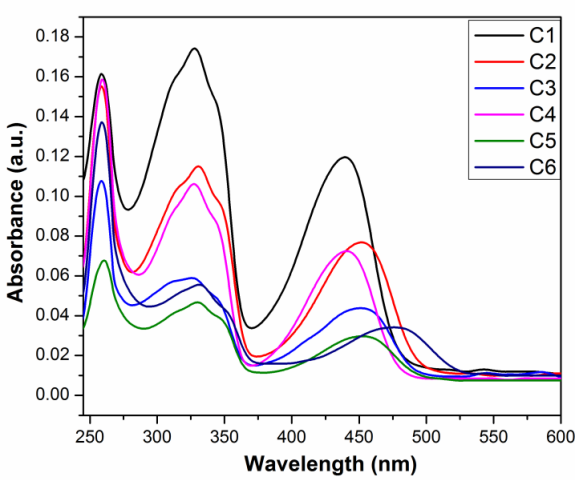

Fig. 2. UV-vis absorption spectra plot of **C1-C6**; 2 mL 10 µM solution of **C1-C6** in chloroform was taken in UV cuvette and subjected to UV-vis analysis

2.1.3. FT-IR spectroscopic study of ***C1-C6***

The FT-IR spectra of **C1-C6** were determined using KBr dilute tableting method and comparative plotted in Fig. 3 and separately plotted in ESI Fig. S19-S24. All the IR spectroscopic signals were assigned according to the previously reported related literature [63], the stretching vibrations of N-H in NH_3 in each **C1-C6** were observed in 3454-3444 cm^{-1} region. The stretching vibration of C=N was assigned in 1642-1637 cm^{-1} region and the broad peak around 1080-1040 cm^{-1} regions was the stretching vibration peak of BF_4 anions, which is also the main difference between **C1-C6** and **SC1-SC6**, confirming that Cl is exchanged with NH_3 [63, 64].

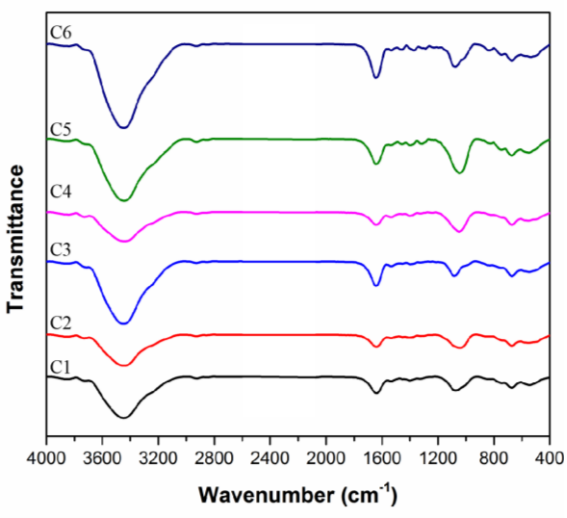

Fig. 3. Comparative FT-IR spectra plot of **C1-C6**

*2.1.4. Single crystal description of **C1, C3, C4** and **C6***

C1, **C3**, **C4** and **C6** were dissolved in CH_2Cl_2 n-hexane solution, and the crystal suitable for single crystal X-ray analysis were obtained by slow evaporation at rt. The structural data were plotted in Fig. 4 - Fig. 7 for (**C1**), (**C3**), (**C4**) and (**C6**) respectively and the structural parameters were listed in Table 1 and 2. **C1** and **C3** belonged to the monoclinic crystal system while **C4** and **C6** belonged to the triclinic crystal system. In all these crystals, the coordination atom ONS came from the main salicylaldimine ligands, O atom was covalently bonded to Pt(II), while SN atoms were coordinate covalently bonded to Pt(II), and the whole coordination assembly was in planar symmetry [66]. The fourth coordinate of Pt(II) in each complex was completed by the co-ligand NH_3 (Fig. 4, 5, 6 and 7). Bond lengths and angles around Pt center in **C1, C3**, **C4** and **C6** were given in Fig. 4B, 5B, 6B and 7B and Table 2. The bond lengths and bond angles in both **C1, C3, C4** and **C6** were almost similar (Table 2 entry 1-4). The longest bond length in **C1**, **C3**, **C4** and **C6** were Pt(1)-S(1) bonds, which were found 2.227(19), 2.326(13), 2.2337(13) and 2.2295(11) Å respectively (Table 2 entry 1), the shortest bond length in **C1** and **C4** was Pt(1)N(1) bond while in **C3** was Pt(1)O(1) bond and in **C6** was Pt(1)N(2) bond (Table 2 entries 2, 3 and 4). In addition, other bond lengths were almost similar. Similarly, the bond angles of the different coordinated atoms of the four complexes at Pt(II) center were almost the same. The biggest bond angles in **C1**, **C3**, **C4** and **C6** were ∠O(1/2)-Pt(1)-S(1), the smallest bond angles of **C1**, **C3** and **C4** were ∠O(1/2)-Pt(1)-N(2), and in **C6** was ∠O(1/2)-Pt(1)-N(1).

There were different interaction between the molecules in the crystal packing of each complex (Fig. 4C, 5C, 6C, 7C), 1D chains were formed by these interaction and further interaction and stacking of 1D

chains formed a three-dimensional arrangement in the crystal packing of each (**C1**, **C3**, **C4** and **C6**) (Fig. 4D, 5D, 6D, 7D).

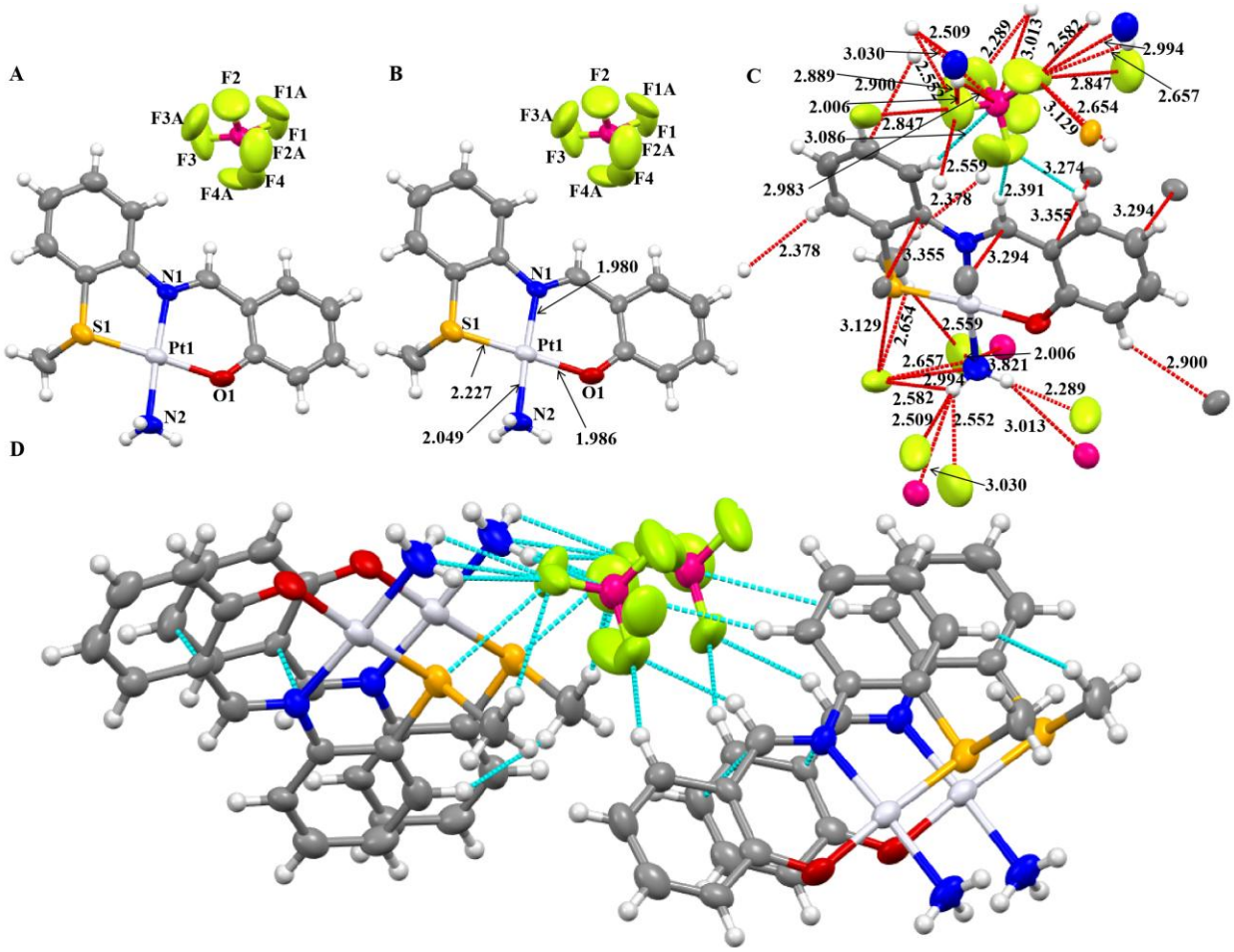

Fig. 4. Single crystal data plot of **C1** at 50% probability of the thermal ellipsoid (A) single molecule showing atoms coordinated with Pt(II) (B) coordination bond lengths (C) plot showing close contacts with neighboring molecules and distances of close contacts (D) 1D chain formation of molecules in crystal packing, the BF4 anions were disordered in this crystal but we showed them as there were mandatory molecular interactions with these anions

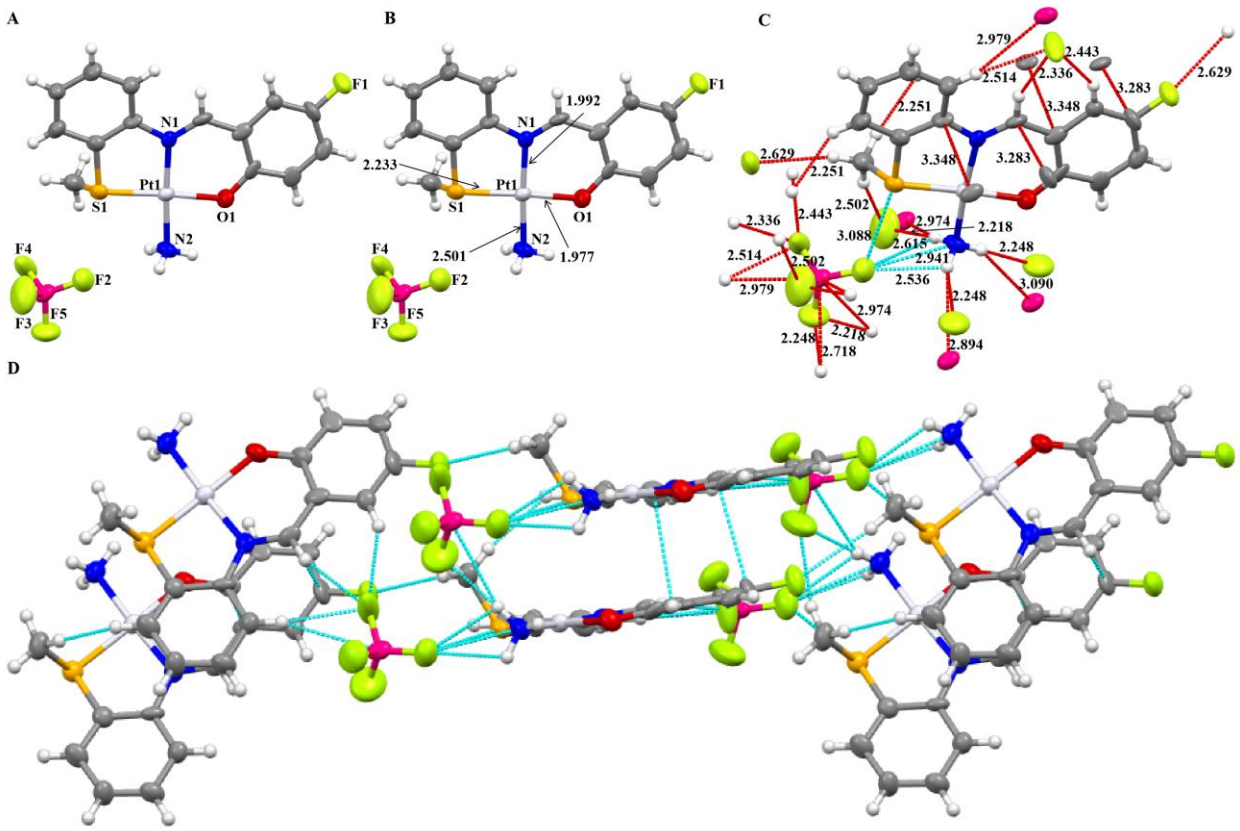

Fig. 5. Single crystal data plot of **C3** at 50% probability of the thermal ellipsoids (A) Molecular plot showing atoms around Pt(II) (B) bond lengths (C) distances of close contacts (D) arrangement of molecules forming 1D chains

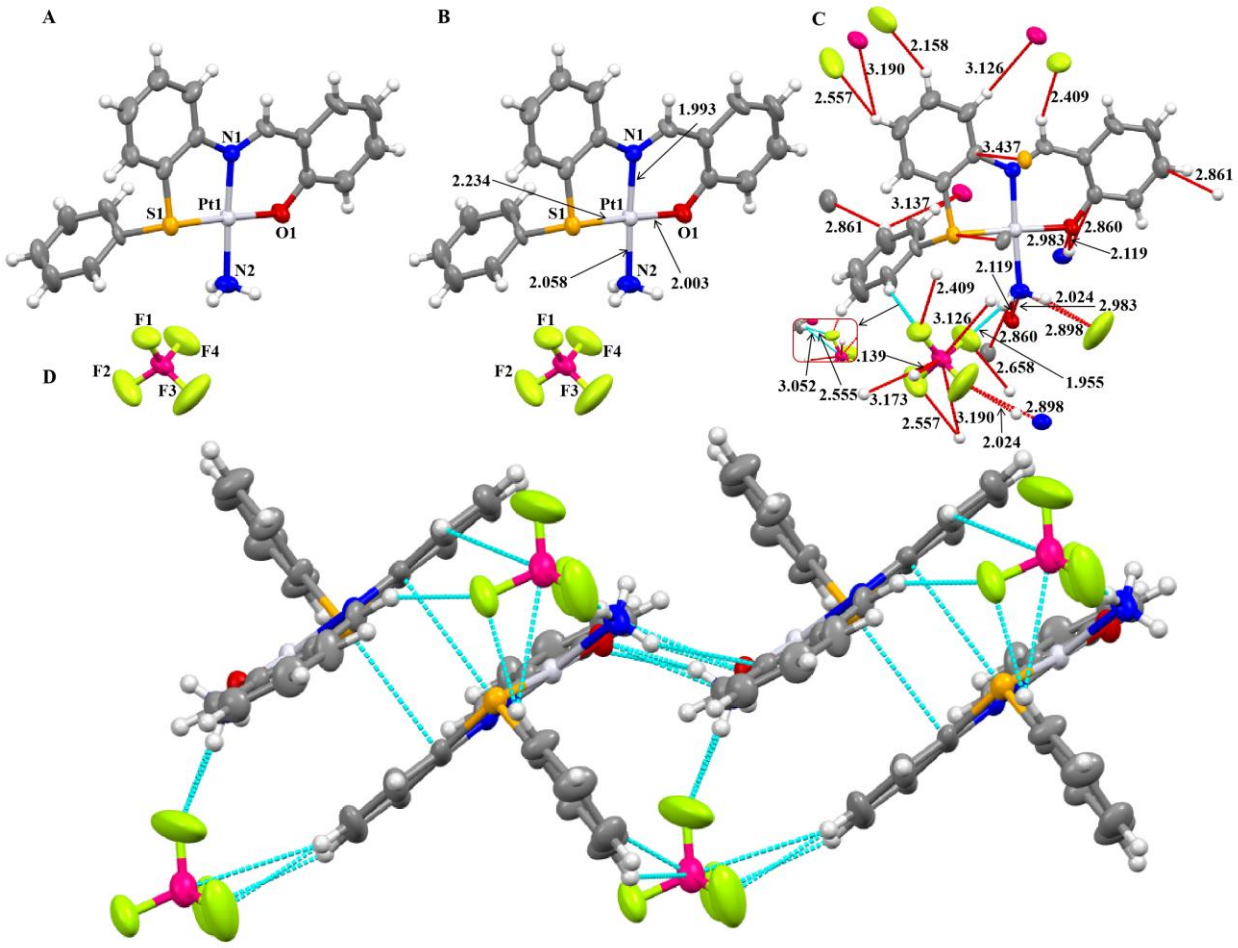

Fig. 6. Single crystal data plot of **C4** at 50% probability of the thermal ellipsoids (A) single molecule plot (B) bond lengths between Pt and other atoms (C) plot showing close contacts lengths with neighboring molecules (D) arrangement of molecules in 1D manner through stacking and close contacts

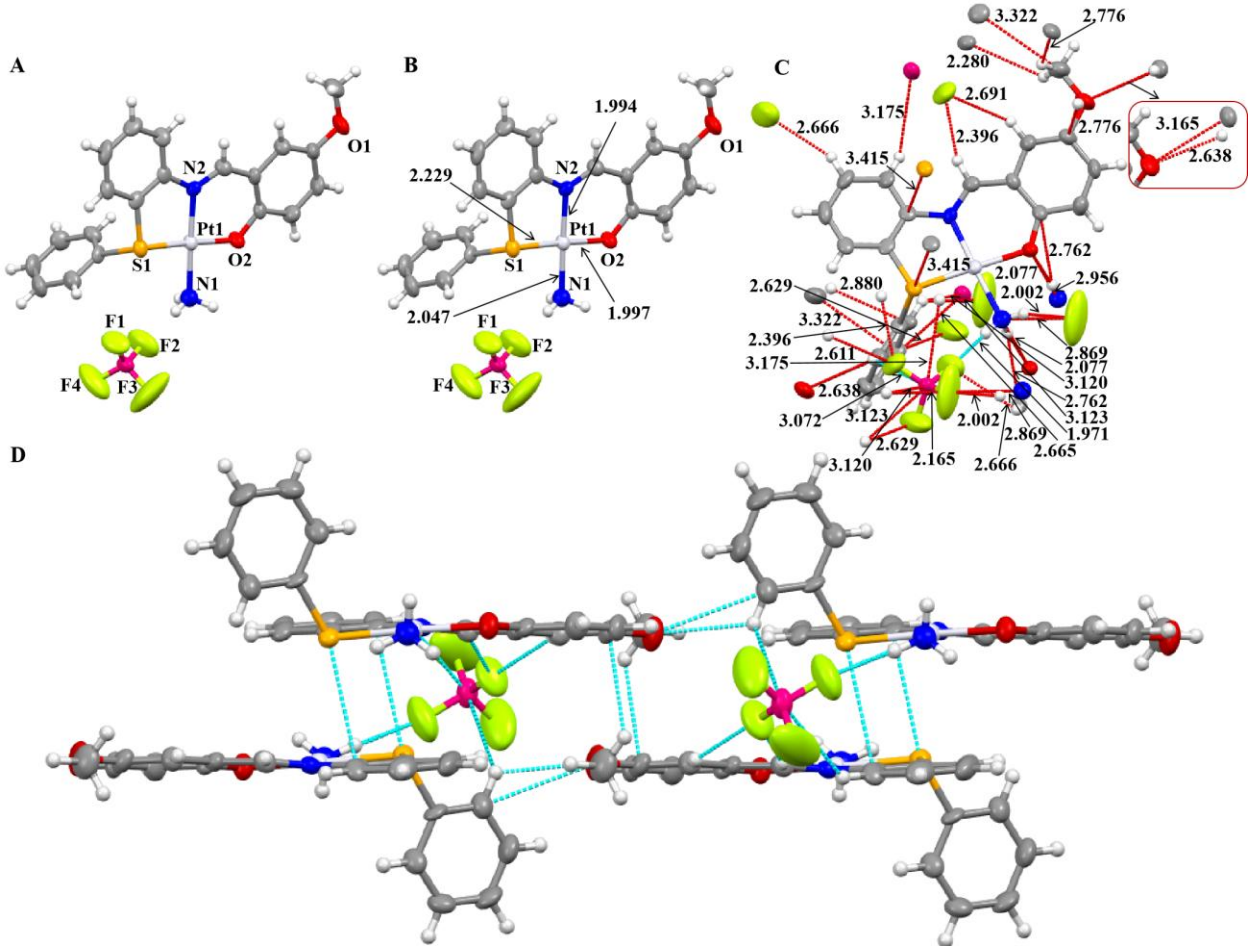

Fig. 7. Single crystal data plot of **C6** at 50% probability of the thermal ellipsoids (A) single molecule plot showing coordinated atoms (B) bond lengths between Pt and other atoms (C) plot showing close contacts lengths (D) arrangement of molecules crystal packing through close contacts or stacking

Table 1 Structure refinement parameters of **C1**, **C3**, **C4**, and **C6**

	C1	**C3**	**C4**	**C6**
Empirical formula	$C_{14}H_{15}BF_4N_2OPtS$	$C_{15}H_{14}BF_5NOPtS$	$C_{19}H_{17}BF_4N_2OPtS$	$C_{20}H_{19}BF_4N_2O_2PtS$
Formula weight	541.24	557.23	603.30	633.33
Temperature (K)	200.00(10)	200.00(10)	293.00(11)	150.00(10)
Crystal system	monoclinic	monoclinic	triclinic	triclinic
Space group	$P2_1/n$	$P2_1/n$	P-1	P-1
Unit cell dimensions	4.9510(3)	4.81391(14)	8.7534(5)	8.8308(5)

a (Å)	17.5429(17)	17.9599(5)	10.7491(6)	10.5735(5)
b (Å)	20.2136(13)	20.0712(6)	11.6744(8)	11.8531(5)
c (Å)	90	90	88.285(5)	89.626(4)
α (°)	92.181(6)	91.066(3)	82.145(5)	83.516(4)
β (°)	90	90	67.495(5)	68.602(5)
γ (°)				
Volume ($Å^3$)	1754.4(2)	1735.00(9)	1004.98(11)	1023.15(9)
Z	4	4	2	2
Density (calculated) (mg/m^3)	2.049	2.133	1.994	2.056
Absorption coefficient (mm^{-1})	8.159	16.769	7.134	7.016
F(000)	1024.0	1052.0	576.0	608.0
Crystal size (mm^3)	0.14 × 0.12 × 0.11	0.15 × 0.11 ×0.09	0.12 × 0.1 × 0.08	0.13 × 0.1 × 0.08
Theta range for data collection (°)	4.644 to 49.986	6.604 to 133.176	4.536 to 50	4.14 to 49.994
Index ranges	$-5 \leq h \leq 5$, $-16 \leq k \leq 20$, $-19 \leq l \leq 24$	$-3 \leq h \leq 5$, $-19 \leq k \leq 21$, $-23 \leq l \leq 22$	$-10 \leq h \leq 10$, $-12 \leq k \leq 10$, $-13 \leq l \leq 13$	$-10 \leq h \leq 10$, $-9 \leq k \leq 12$, $-14 \leq l \leq 14$
Reflections collected	7394	5824	7391	6732
Independent reflections	3071 [Rint = 0.0414, Rsigma = 0.0649]	3066 [Rint = 0.0620, Rsigma = 0.0751]	3540 [Rint = 0.0520, Rsigma = 0.0672]	3598 [Rint = 0.0335, Rsigma = 0.0577]
Data / restraints / parameters	3071/64/256	3066/0/228	3540/0/263	3598/0/282
Goodness-of-fit on F^2	0.957	1.062	0.979	1.019
Final R indices [I>2sigma(I)]	$R_1 = 0.0360$ $wR_2 = 0.0644$	$R_1 = 0.0838$, $wR_2 = 0.2442$	$R_1 = 0.0295$, $wR_2 = 0.0570$	$R_1 = 0.0266$, $wR_2 = 0.0453$

R indices (all data)	R_1 = 0.0531, wR_2 = 0.0711	R_1 = 0.0939, wR_2 = 0.2636	R_1 = 0.0340, wR_2 = 0.0608	R_1 = 0.0307, wR_2 = 0.0577
Largest diff. peak and hole (e.Å^{-3})	0.16/-0.62	1.62/-1.32	0.73/-1.13	1.13/-1.11

Table 2. Selected bond lengths (Å) and angles (°) around Pt atom in each **C1**, **C3**, **C4** and **C6**

Entry	Bond/Angle	**C1**	**C3**	**C4**	**C6**
Bond length (Å)					
1	Pt(1)-S(1)	2.2270(19)	2.3264(13)	2.2337(13)	2.2295(11)
2	Pt(1)-O(1/2)	1.986(5)	1.977(10)	2.003(3)	1.997(3)
3	Pt(1)-N(1)	1.981(5)	1.992(12)	1.993(4)	2.047(3)
4	Pt(1)-N(2)	2.050(6)	2.052(12)	2.057(4)	1.994(3)
Bond angle (°)					
5	∠O(1/2)-Pt(1)-S(1)	176.97(15)	177.5(3)	177.10(11)	176.86(8)
6	∠O(1/2)-Pt(1)-N(1)	95.1(2)	95.0(5)	94.32(16)	83.06(13)
7	∠O(1/2)-Pt(1)-N(2)	81.9(2)	81.4(5)	83.73(16)	95.09(12)
8	∠N(1)-Pt(1)-S(1)	87.27(16)	87.0(3)	87.26(13)	94.69(10)
9	∠N(1)-Pt(1)-N(2)	177.0(2)	176.3(5)	177.59(17)	177.99(13)
10	∠N(2)-Pt(1)-S(1)	95.70(18)	96.7(4)	94.62(12)	87.14(10)

2.1.5. Stability in solution state studied by ^{1}H NMR spectroscopy

The stability of a platinum complex is a crucial factor affecting its biological activity. For *in vitro* biological experiments, the drug solution in most of the cases is prepared in DMSO, some time the donor ligands were easily replaced by DMSO that altered the structure of the Pt complex and in turn affected the

antitumor efficacy [67-68]. At the same time, based on the antitumor mechanism of platinum complexes, the first step to activate Pt complex was to form H_2O-Pt(II) hydrate. Based on the above two points, the stability of platinum complexes used as an antitumor drug candidate is important to be measured in DMSO and H_2O [69]. We also studied the stability by repeated time-dependent ^{1}H NMR spectroscopic analysis. **C1** was used as a reference complex and time dependent ^{1}H NMR analyses were performed in DMSO-d_6 (ESI Fig. S25). As these complexes were insoluble in pure water so we selected 15%D_2O/DMSO-d_6 as solvent to check the effect of presence of water on the stability of **C1**, time-dependent repeated ^{1}H NMR spectroscopic analyses were performed (ESI Fig. S26). These analyses conducted over 7 days showed no changes in the main protons chemical shifts of **C1** in these two different media. It is confirmed that **C1** has high stability in these media and could prove a potential anticancer agent.

2.2. Biology

2.2.1. Inhibition of the growth ability of TNBC cells

TNBC is one of the most aggressive subtypes of breast cancer, and chemotherapy is the main treatment [70-71]. We selected three TNBC cell lines including MDA-MB-231, MDA-MB-468 and MDA-MB-436 to determine the cytotoxicity of **C1-C6**. These breast cancer cells were treated with 20 μM of each **C1-C6** or doxorubicin (Dox) for 48 hours, and the cell growth rate was measured. MTT assays results showed that **C4** and **C6** had obvious cytotoxicity in these three types of cancer cells (Fig. 8 A-C). These two complexes had the potential to inhibit the growth of three malignant breast cancer cells, among these **C4** had the strongest cytotoxicity. Based on this, we examined the relationship between the cytotoxicity and dose of **C4** on three types of breast cancer cells (Fig. 8 D-F). MTT assays results showed that compared with CTL, **C4** inhibited the growth cancer cells in concentration dependent manner, it showed cytotoxicity at 2.5 μM level that was further higher for higher concentration of **C4** and 15 μM was sufficient to inhibit the growth of these cancer cells. These results indicated that **C4** has a strong inhibitory effect on the growth of MDA-MB-231, MDA-MB-468 and MDA-MB-436 breast cancer cells and may be a key complex in the this group of six complexes. We have performed MTT assay in MCF-10A cells treated with different concentrations of **C4** and our results show that **C4** was less cytotoxic in normal (MCF-10A) cells (ESI Fig. S32).

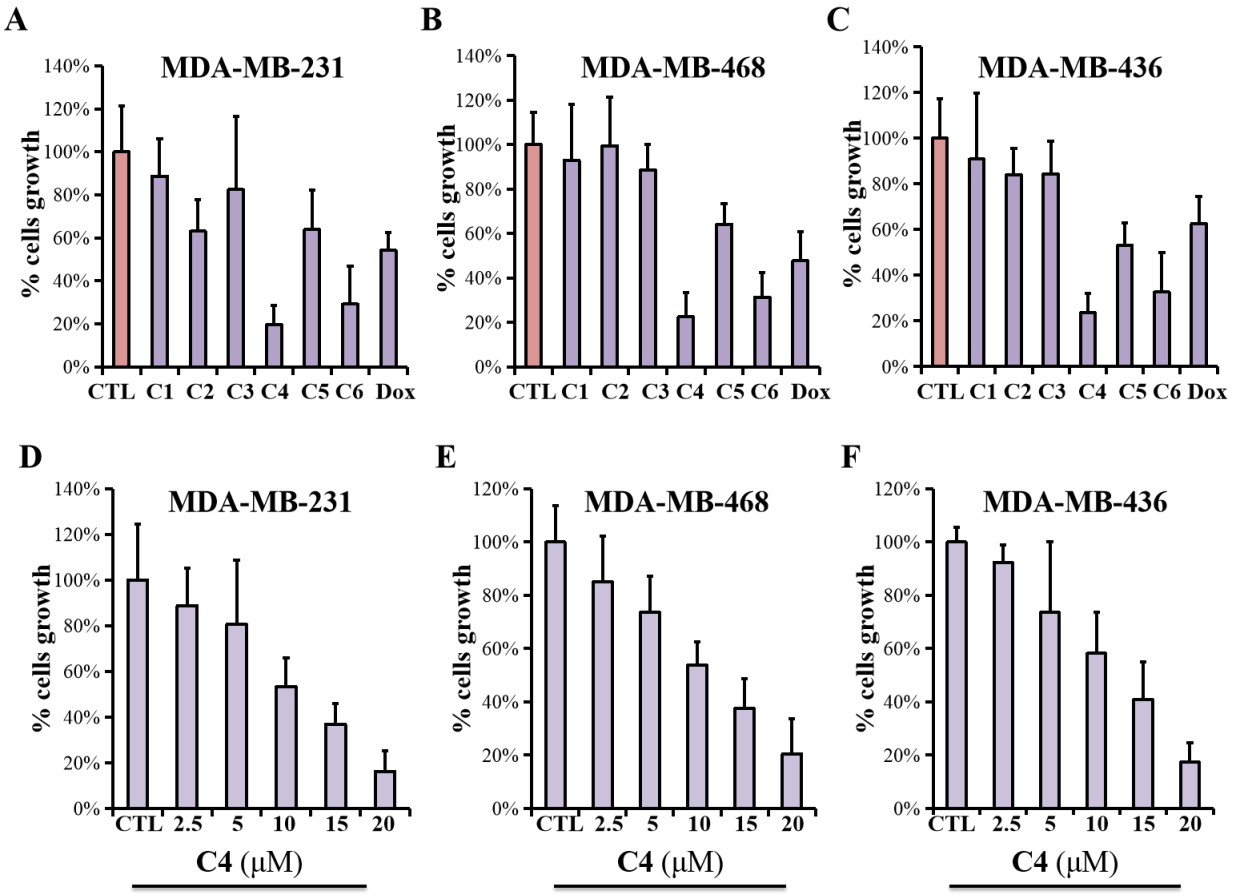

Fig. 8. C1-C6 inhibited the proliferation of MDA-MB-231, MDA-MB-468 and MDA-MB-436 breast cancer cells; **(A-C)** MDA-MB-231, MDA-MB-468 and MDA-MB-436 breast cancer cells were treated with 20 μM of each **C1-C6** and positive control doxorubicin (Dox) for 48 h, and the cell growth rate was measured. CTL represented DMSO treatment. **(D-F)** MDA-MB-231, MDA-MB-468 and MDA-MB-436 breast cancer cells were treated with CTL, 2.5, 5, 10, 15 and 20 μM of **C4** for 48 h and cell growth rate was measured by MTT assays

*2.2.2. Comparison of cytotoxic effect of **C4** with standard chemotherapeutic agents*

We compared the cytotoxicity of **C4** and commonly used chemotherapeutic drugs cisplatin, oxaliplatin and 5-fluorouracil (5-FU) on MDA-MB-231, MDA-MB-468 and MDA-MB-436 breast cancer cells by MTT assay (Fig. 9 A-C). The results showed that **C4** had the strongest inhibitory effect on the growth of cancer cells, and the cytotoxicity effect was stronger than that of cisplatin, oxaliplatin and 5-FU. These results demonstrated that **C4** may be a potential antitumor drug for the treatment of MDA-MB-231, MDA-MB-468 and MDA-MB-436 breast cancers.

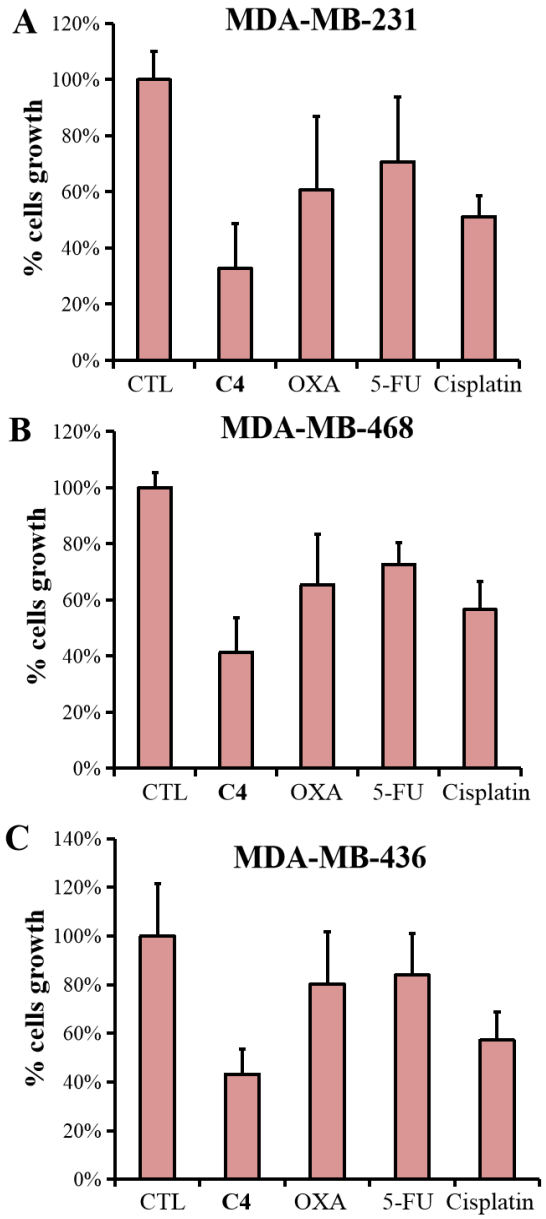

Fig.9. Comparison of cytotoxicity of **C4** with market available anticancer drugs; **(A-C)** MDA-MB-231, MDA-MB-468 and MDA-MB-436 cells were treated with 10 μM of each **C4**, cisplatin, oxaliplatin (OXA) or 5-fluorouracil (5-FU) for 48 h, and the cell growth rate was measured. CTL represented DMSO treatment

*2.3.3 Effect of **C4** on clonogenic potential of triple-negative-breast cancer cells*

The survival, metastasis and drug resistance of cancer cells are closely related to the clone formation ability of cancer cells [72]. We examined the effect of **C4** on the colony formation ability of MDA-MB-231, MDA-MB-468 and MDA-MB-436 breast cancer cells (Fig. 10 A-C). The cancer cells were treated

with DMSO, 2.5 and 5 μM **C4** for 7 days and analysed. The purple color of the cancer cells culture dishes treated with 2.5 or 5 μM of **C4** was significantly lighter as compared to the DMSO treated cells, and the relative absorbance was significantly decreased, indicating that **C4** has the ability to inhibit the colony formation of MDA-MB-231, MDA-MB-468 and MDA-MB-436 cells.

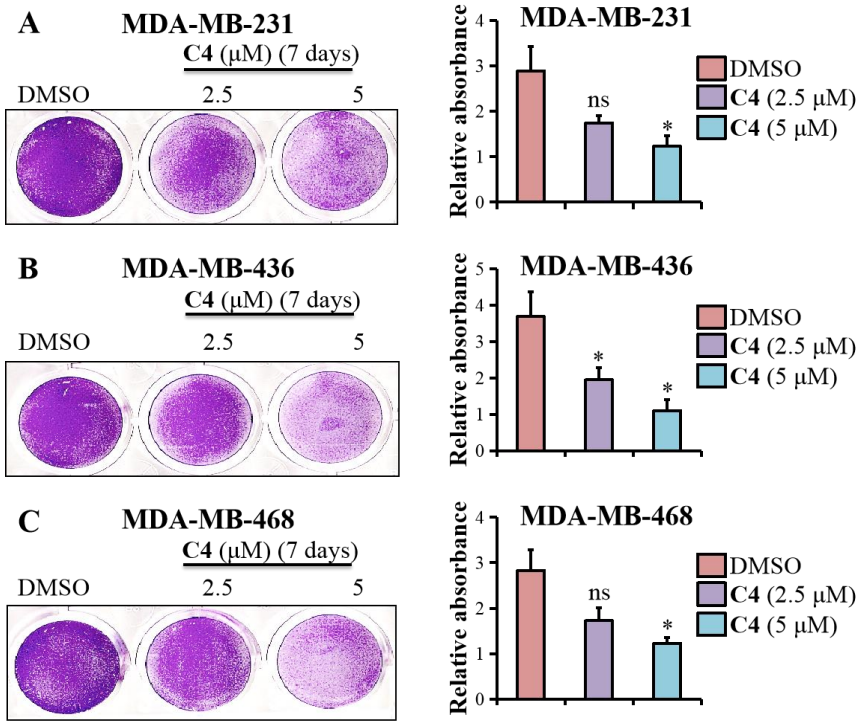

Fig. 10. The effect of **C4** on the clone formation ability of TNBC cells; **(A-C)** MDA-MB-231, MDA-MB-468 and MDA-MB-436 breast cancer cells were treated with DMSO, 2.5 or 5 μM of **C4** for 7 days and clonogenic potential was determined using crystal violet staining assay. Color intensity reflected cell viability. Statistical analysis represents student t-test *p < 0.05; **p < 0.005; ***p < 0.0005. ns means non-specific

*2.2.4. **C4** inhibited the invasion ability of different TNBC cells*

Cancer cells fall off from the primary site, first causing canceration of surrounding tissues called invasion. Invasive cancer cells further migrate to other new tissues and organs, eventually leading to cancer cell metastasis. Therefore, inhibition of cancer cell invasion inhibits cancer cell metastasis [73]. MDA-MB-231, MDA-MB-468 and MDA-MB-436 breast cancer cells were treated with 10 μM **C4** for 48 h, and the invasion ability of cancer cells was determined by transwell chamber cancer cell invasion assay. The results showed that compared with the control cells treated with DMSO (Fig. 11), the blue color of cancer cells treated with **C4** was significantly lighter, and the relative number of invasive cells was significantly

reduced, indicating that **C4** had a strong ability to inhibit the invasion of MDA-MB-231, MDA-MB-468 and MDA-MB-436 cells.

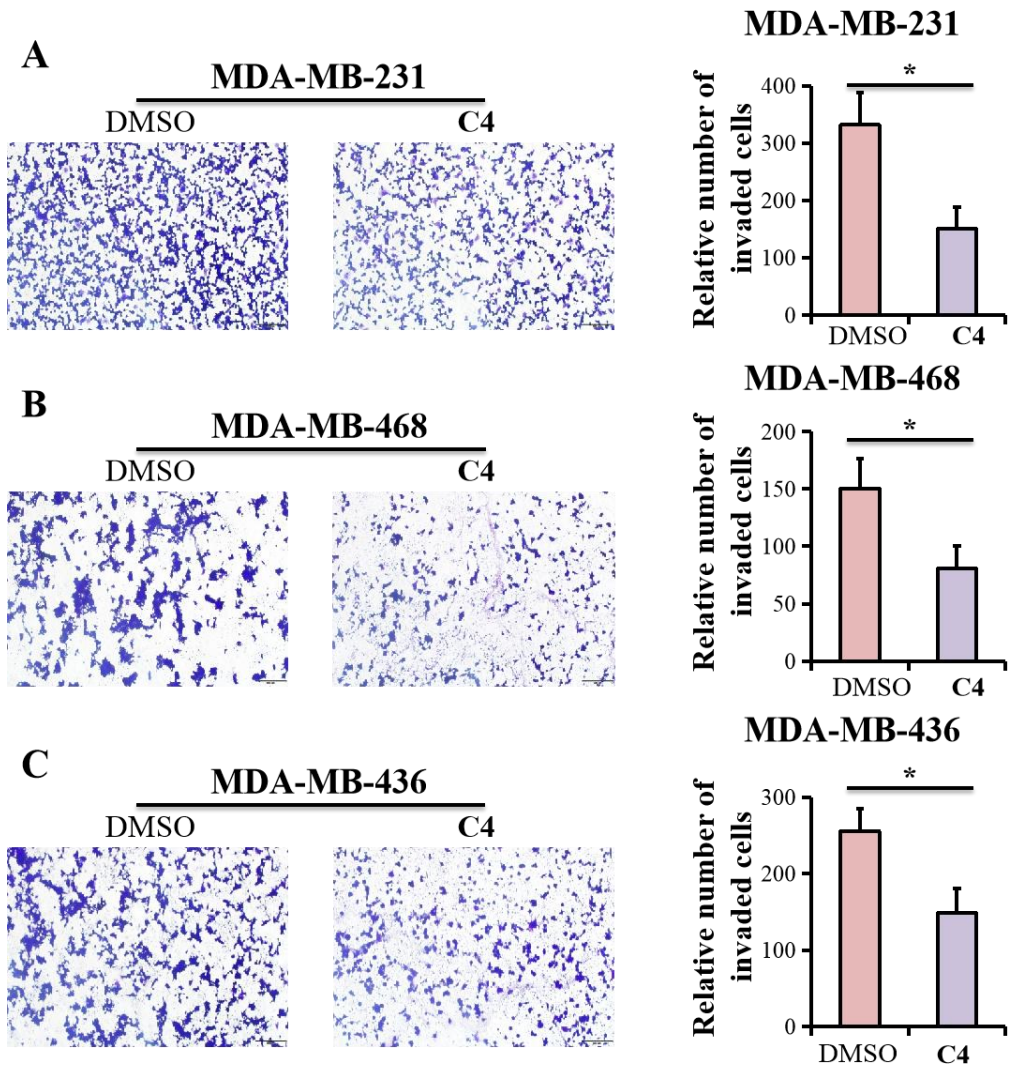

Fig. 11. Cancer cells invasion study; **(A-C)** MDA-MB-231, MDA-MB-468 and MDA-MB-436 cells were treated with control (DMSO), or 10 μM of **C4** for 48 h and invasion ability was determined by cell invasion assay (Magnification 20×). Statistical analysis represents student t-test *$p < 0.05$

*2.2.5. Tumor spheroids formation suppression by **C4** in triple-negative-breast cancer cells*

Tumor stem cell formation promotes tumor development, metastasis and drug resistance [74]. We examined the effect of **C4** on mammopshere formation/stem cell formation (Fig. 12). MDA-MB-231, MDA-MB-468 and MDA-MB-436 breast cancer cells were cultured as breast cancer stem cells, and then treated with 5 μM **C4** for 7 days. The sphere formation experiment can be visually observed, compared

with the DMSO-treated control group, the stem cell sphere formation ability of the cancer cells in the **C4** treated group was significantly reduced, indicating that **C4** has the ability to inhibit the formation of MDA-MB-231, MDA-MB-468 and MDA-MB-436 cancer stem cells and there by blocking cancer progression.

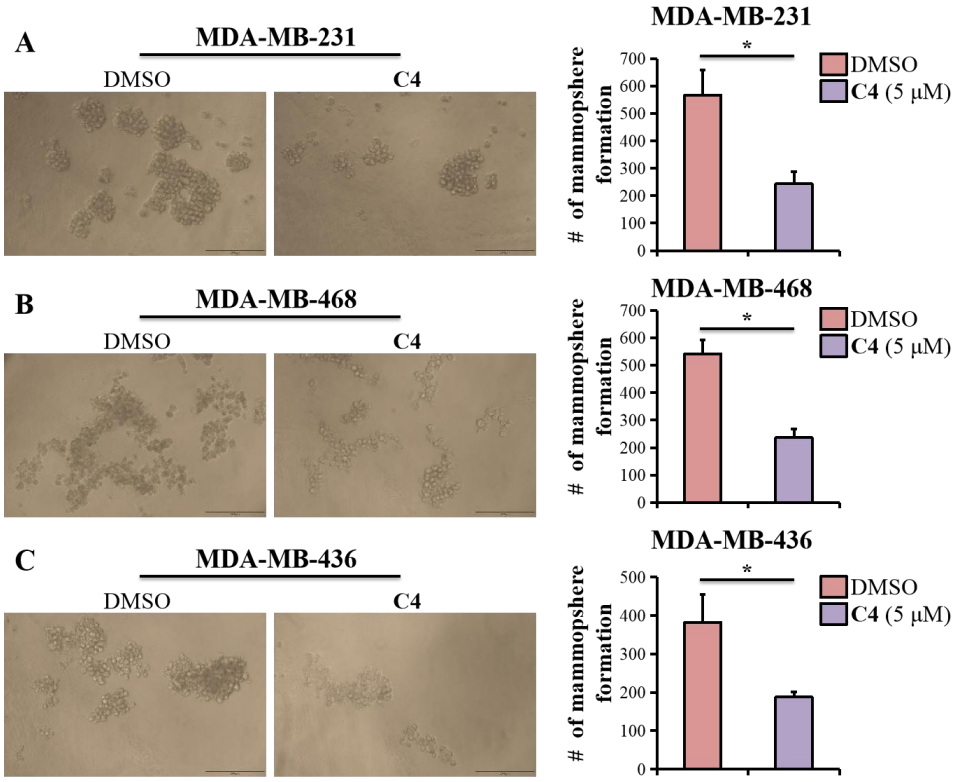

Fig.12. C4 inhibited the formation of mammopshere in three TNBC cells; **(A-C)** MDA-MB-231, MDA-MB-468 and MDA-MB-436 breast cancer cells were grown as spheroids, treated with DMSO and **C4** (5 µM) for 7 days and the effect of **C4** on the formation of mammopshere was determined. Statistical analysis represents student t-test *p < 0.05

*2.2.6. **C4** synergized anticancer effect with palbociclib, JQ1 and paclitaxel in TNBC cells*

As a CDK4/6 inhibitor, palbociclib has been approved for the treatment of breast cancer, but TNBC is more resistant to palbociclib [75]. JQ1 is a bromodomain and extra-terminal domain (BET) inhibitor, which is a promising therapeutic drug for TNBC [76]. Paclitaxel (a microtubule-inhibiting chemotherapy) is the first-line chemotherapy drug for TNBC, but it increases cancer stem-like cells (CSCs) in residual tumors [77]. Based on mechanism, platinum drugs acting as DNA targeted drugs, the potential of **C4** in the field of combined use was discussed by combining it with other chemotherapy drugs acting through other mechanisms such as palbociclib, JQ1 and paclitaxel. We examined the effects of **C4** combined with

palbociclib, JQ1 and paclitaxel on the growth of MDA-MB-231 and MDA-MB-436 breast cancer cells (Fig. 13 A-F). Obviously, when these four drugs were used alone, cell growth was inhibited to a certain extent compared with the control group. However, when **C4** was combined with palbociclib, JQ1, and paclitaxel, the cell growth inhibition was significantly enhanced, and the inhibition of cell proliferation was stronger. It was proved that the combination of **C4** with palbociclib, JQ1 and paclitaxel had a synergistic anticancer effect and induced more cancer cell death. In combination with palbociclib, JQ1 and paclitaxel, **C4** exerts an effective synergistic anticancer effect, and the inhibitory effect on tumor cell growth is greatly enhanced.

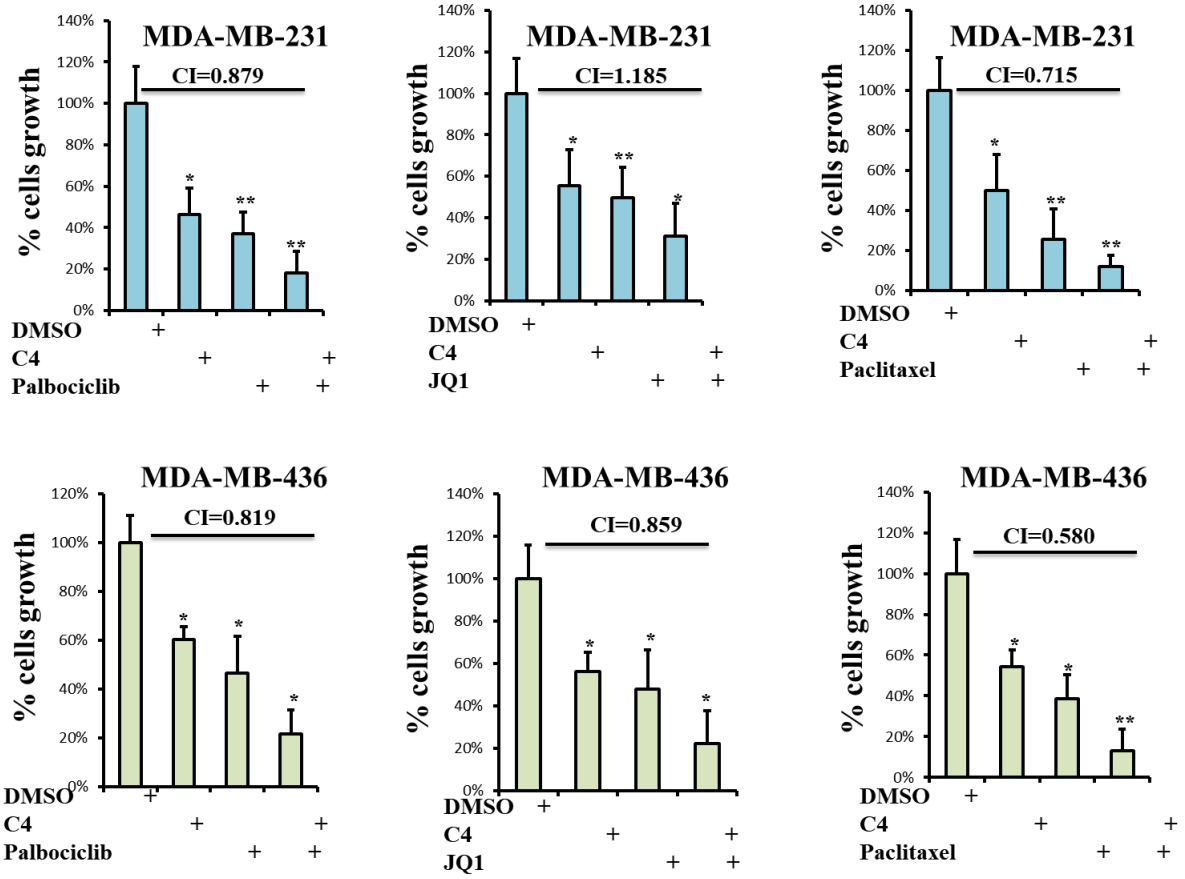

Fig. 13. C4 synergized anticancer effect in combination with palbociclib, JQ1 or paclitaxel in triple-negative-breast cancer cells; To study the combined effect of **C4** and palbociclib, **C4** and JQ1 and **C4** and paclitaxel in MDA-MB-231 and MDA-MB-436 breast cancer cells, cancer cells were treated with DMSO, 10 μM **C4**, 2.5 μM palbociclib, 5 μM JQ1 and 20 nM paclitaxel alone or in combination for 48 h and cell viability was measured by MTT assay, Drug combination index (CI) was calculated according to the method described by Chou–Talalay. CI < 1 synergism, CI = 1 additive effect and CI > 1 antagonism.

Statistical analysis was performed using unpaired student t test. P<0.05*, P < 0.005** was considered statistically significant.

*2.2.7. **C4** inhibited TNBC cell cycle progression by targeting the expression of MYC/STAT3/CCND1/CNNE1/p27.*

Transcription factors (TFs) are a class of proteins that have DNA binding domains in the promoter or enhancer regions of specific genes [78]. Cell cycle-related TFs can be used as potential targets for tumor therapy. Transcriptional modulators MYC (include C-MYC, L-MYC and N-MYC) belong to the superfamily of basic helix-loop-helix leucine zipper (bHLHLZ) DNA binding proteins [79]. MYC regulates overall gene expression, thereby promoting proliferation and many other cellular processes [80]. Interestingly, MYC not only promotes the transcription of the oncogenic proteins, but also suppresses the transcription of tumor suppressor genes [81]. In addition, MYC can also inhibit the recruitment and activation of immune cells in TNBC by inhibiting the transcription of interferon genes [82]. STAT3 is a transcription factor protein that regulates gene expression related to cell cycle progression, cell survival, and immune response in cancer cells. Once activated, STAT3 forms a homodimer, enters the nucleus and binds to DNA, promoting the translation of target genes related to anti-apoptosis, angiogenesis, invasion and migration [83-84]. Cyclin D1 (CCND1) and Cyclin E1 (CNNE1), as cell cycle regulators, cyclin can form complex with CDK to promote cell cycle from the first growth G1 to DNA synthesis S phase and promote cell proliferation [85-88]. They play an important role in TNBC cell growth, cell cycle regulation and migration [89-91]. The transcription and translation of MYC and cyclin can activate STAT3 signaling pathway and promote cell cycle progression [92]. CDKN1B gene encodes p27 is a widely expressed cell cycle inhibitor that blocks cell cycle by binding and inhibiting cyclin-dependent kinase (CDK) [93]. MDA-MB-231 and MDA-MB-436 cells were treated with 10 μM **C4** for 2 days. RT-PCR was performed to detect the expression of cell cycle markers MYC/STAT3/CCND1/CNNE1/p27 (Fig. 14). Obviously, cancer cells treated with **C4**, the cell cycle progression markers including MYC/STAT3/CCND1/CNNE1 were down-regulated, while the expression of P27 was up-regulated, demonstrating that **C4** strong potentials to inhibit cancer cell proliferation and cycle progression.

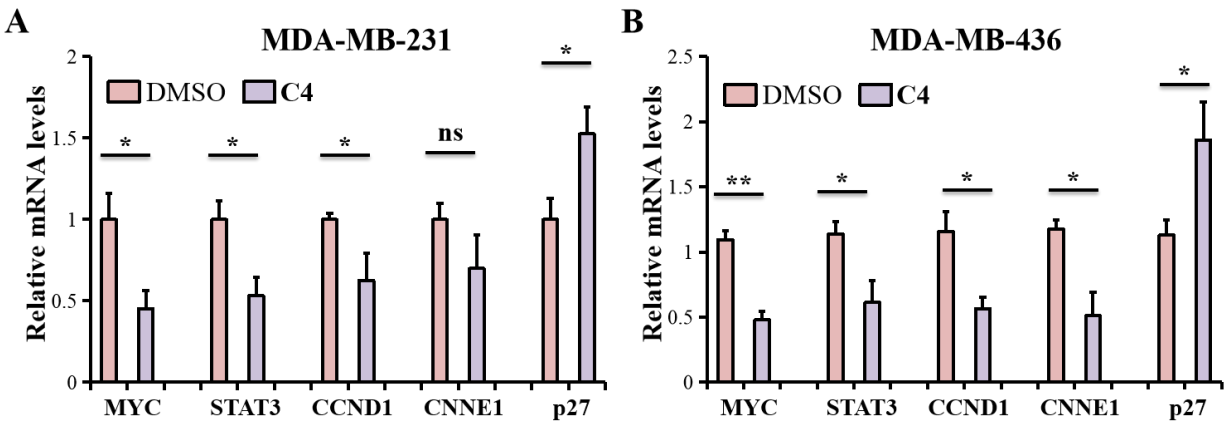

Fig. 14. C4 targeted MYC, STAT3, CCND1, CNNE1 and p27 in triple-negative-breast cancer cells; MDA-MB-231 and MDA-MB-436 cells were treated with **C4** (10 μM) for 48 h and MYC/STAT3/CCND1/CNNE1/p27 expressions were determined by RT-PCR. Statistical analysis represents student t-test *$p < 0.05$; **$p < 0.005$; ***$p < 0.0005$. ns means non-specific

*2.2.8. **C4** inhibited TNBC cell proliferation by targeting CDK4/6 expression*

CDK4/6 is a key regulator of the cell cycle [94], overactivity leads to excessive proliferation of tumor cells and accelerates the transition of the cell cycle from the first growth (G1) to the DNA synthesis (S) stage [95-96]. CDK4/6 inhibitors block the cell cycle in G1 phase, leading to DNA double-strand damage and blocking the proliferation of invasive tumor cells [97]. Some preclinical experiments and clinical trials have shown the therapeutic effect of CDK4/6 inhibitors on TNBC, the combination therapy may help overcome drug resistance by targeting multiple signaling pathways in TNBC [98]. Therefore, we investigated the effect of these complexes on CDK4/6 expression. MDA-MB-231, MDA-MB-468 and MDA-MB-436 cells were treated with 10 μM of **C4** for 2 days and cell cycle progression marker CDK4/6 expression was determined by western blot (Fig. 15). Western blot data showed inhibition of CDK4/6 expression in cells treated with **C4** as compared to control cells. Importantly, the inhibition of CDK4/6 expression by **C4** was much stronger in MDA-MB-231 cells which suggested the importance of **C4** in breast cancer cells. These results suggest that **C4** caused DNA damage by inhibiting the activity of CDK4/6, inhibited the proliferation of tumor cells and reduced the invasion ability of cancer cells.

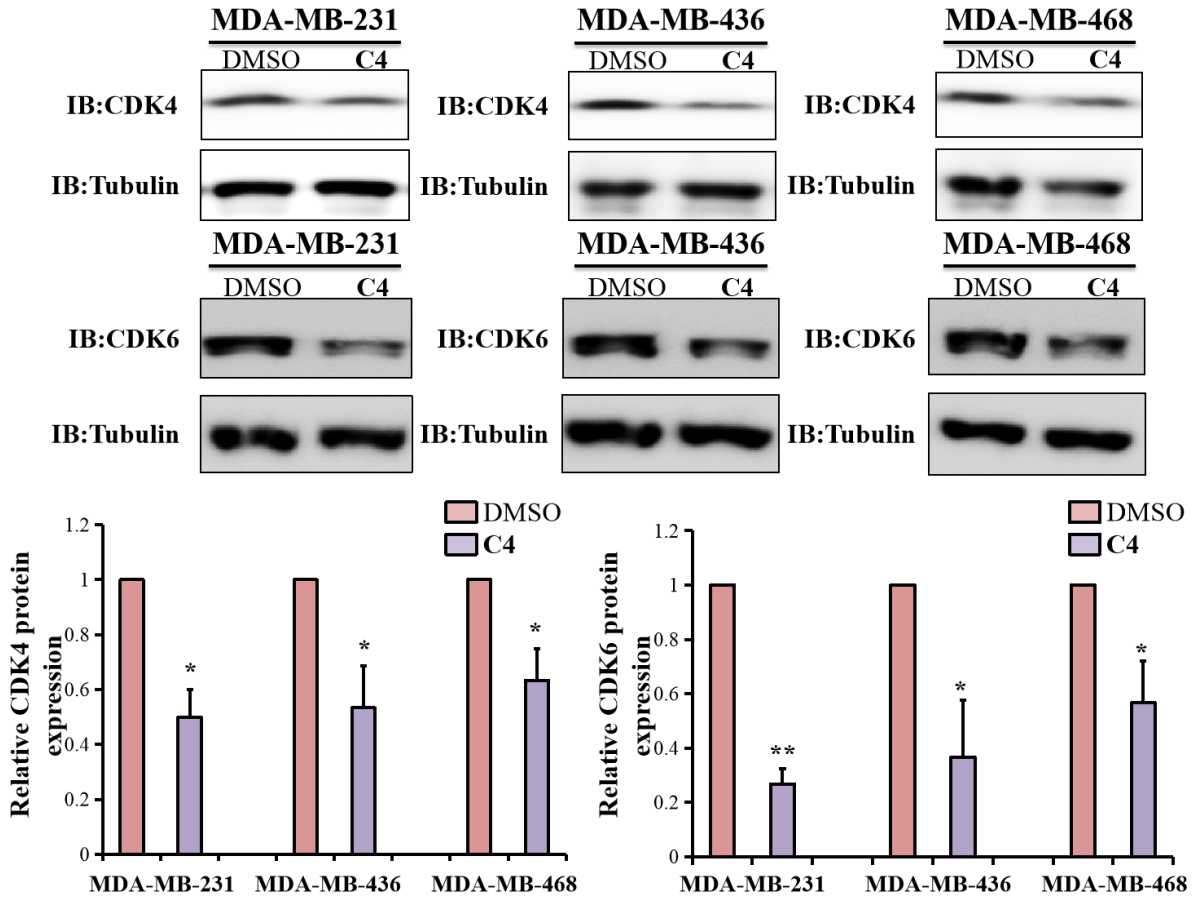

Fig. 15. C4 targeted CDK4/6 axis in triple-negative-breast cancer cells; MDA-MB-231, MDA-MB-468 and MDA-MB-436 cells were treated with **C4** (10 μM) for 2 days and CDK4/6 expression was determined by western blot. Tubulin was used as a loading control. Statistical analysis represents student t-test *p < 0.05; **p < 0.005; ***p < 0.0005

*2.2.9. **C4** suppressed epithelial-mesenchymal transition (EMT) expressions*

Epithelial-mesenchymal transition (EMT) plays an important role in the invasion and metastasis of breast cancer cells. Through EMT, cancer cells can obtain higher invasion and migration ability. Inhibition of EMT may be an effective way to inhibit breast cancer metastasis [99]. Mesenchymal proteins Twist-related protein 1 (TWIST1), zinc finger protein SLUG (SLUG) and Zinc-finger E-box binding homebox 1 (ZEB1) promote the mesenchymal transition by inhibiting the expression of E-cadherin, thereby causing the disintegration of cell-cell adhesion and inducing EMT [100-101]. As a key biomarker of EMT, vimentin is expressed in mesenchymal cells and is up-regulated during tumor metastasis [102]. E-cadherin and tight junction protein ZO-1 (TJP1) are epithelial marker proteins in the process of EMT, which are the key components to inhibit tumor invasion and metastasis, the expression of ZO-1 is down-

regulated in EMT [103-105]. Therefore, we investigated the effect of **C4** on TWIST1/SLUG/ZEB1/VIM/ZO-1 expressions. MDA-MB-231 cells were treated with 10 μM of **C4** for 2 days and EMT markers TWIST1/SLUG/ZEB1/VIM/ZO-1 expression was determined by RT-PCR (Fig. 16). RT-PCR data showed inhibition of TWIST1/SLUG/ZEB1/VIM expression and enhanced ZO-1 expression in cells treated with **C4** as compared to control cells. These results suggested the importance of **C4** in killing cancer cells, thereby inhibiting the EMT process and reducing the invasion and metastasis of cancer cells.

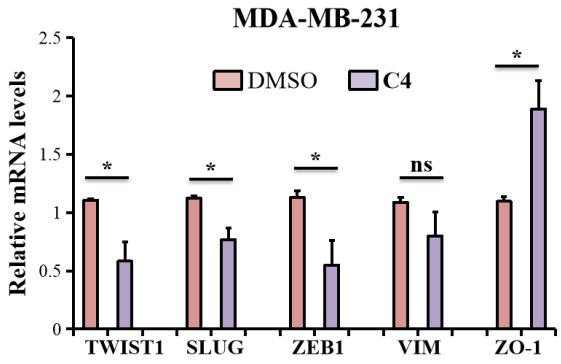

Fig. 16. Effect of **C4** on EMT in triple-negative-breast cancer cells; MDA-MB-231 cells were treated with 10 μM of **C4** for 2 days. TWIST1, SLUG, ZEB1, VIM and ZO-1 expressions were determined by RT-PCR. Statistical analysis represents student t-test *$p < 0.05$; **$p < 0.005$; ***$p < 0.0005$

3. Discussion

Chemotherapy is a popular and successful method of cancer treatment, after cisplatin is approved as an chemotherapeutic drug in clinical practices, platinum drugs have attracted much attention in the field of anticancer drug research, but they were often accompanied by serious side effects and severe drug resistance, which limited the use of platinum drugs [106]. Cisplatin has been widely used in the treatment of cancer, but its efficacy is indeed affected by adverse reactions and drug resistance. Although transplatin has been neglected because it did not show anticancer activity, it has been found that its derivatives have excellent anticancer activity against a variety of cancers [57].

Based on this, we synthesized **C1-C6** with SNO donor salicylaldimine ligands bearing different functions and NH_3 co-ligand at *trans*-position by a simple and efficient method and characterized them by detailed structure elucidation techniques. The exact assembly of the ligands and Pt(II) in solid state was studied by single crystal X-ray analysis. Similarly, we analyzed their stability in solution using NMR methods. The

in vitro anticancer activity results showed that they have excellent anti-TNBC activities through multiple mechanistic pathways.

TNBC is a subtype of malignant breast cancer with extensive heterogeneity, high metastasis rate, severe chemotherapy resistance, poor clinical effect, high recurrence rate and adverse prognosis [107]. Chemotherapy as an important method for the treatment of TNBC faces enormous challenges, and it is urgent to develop new chemotherapy drugs to alleviate this situation [108].

We carried out a detailed *in vitro* antitumor activity analyses, firstly, the antitumor activity on three selected TNBC cell lines including MDA-MB-231, MDA-MB-468 and MDA-MB-436 was tested. All these complexes showed good cytotoxicity in these cancer cells. **C4** inhibited cell growth most obviously and had the best cytotoxic effect in a dose-dependent manner. Next, **C4** was compared with cisplatin, oxaliplatin and 5-FU, we found **C4** had better antitumor activity as compared to these drugs. In addition, **C4** has the ability to inhibit the colony formation of MDA-MB-231, MDA-MB-468 and MDA-MB-436 breast cancer cells and inhibited the invasion and metastasis of cancer cells. At the same time, **C4** also inhibited the generation of tumor stem cells, inhibited the progress of tumor cells and showed a good synergistic antitumor effect when combined with palbociclib, JQ1 and paclitaxel respectively. These results confirmed the potential of **C4** in the field of anti-TNBC. Based on the above performance of **C4** in anti-TNBC, we further explored the specific mechanism of **C4** regulating tumor cell invasion, stemness, and cell cycle progression. Mechanistically, MYC/STAT3/CCND1/CNNE1/p27 are cell cycle-related proteins, MYC/STAT3/CCND1/CNNE1 are positive regulators of cell cycle while p27 is a negative regulator of cell cycle. In the process of cancer cell cycle MYC/STAT3/CCND1/CNNE1 is up-regulated, while p27 is down-regulated. RT-PCR was used to detect the expression of these cell cycle markers in cancer cells treated with **C4**, and the down-regulation of the positive regulator MYC/STAT3/CCND1/CNNE1 was observed, while P27 was just the opposite, indicating that **C4** inhibits cell cycle progression and inhibits cancer cell proliferation by targeting MYC/STAT3/CCND1/CNNE1/p27. CDK4/6 is a cyclin-dependent kinase that forms complexes with cyclins (MYC/STAT3/CCND1 etc.) during cell cycle progression, thereby promoting the transition of cell cycle progression from G1 phase to S phase. However, when TNBC was treated with **C4**, the expression of CDK4/6 was observed to be inhibited compared with the control group, thereby affecting the cell cycle progression, which was consistent with the expression of the above cell cycle-related proteins. It is indicated that **C4** regulated the expression of MYC/STAT3/CCND1/CNNE1/p27 by inhibiting the expression of CDK4/6, thereby inhibited the cell cycle process of cancer cells, inhibited the proliferation of cancer cells and reduced their ability to invade.

The occurrence of EMT increases the motivation for the invasion and migration of cancer cells. In this process, the expression of TWIST1/SLUG/ZEB1/VIM protein is increased, while the expression of another marker ZO-1 is inhibited. The expression of TWIST1/SLUG/ZEB1/VIM was significantly down-regulated in MDA-MB-231 cells treated with **C4**, while the expression of ZO-1 was up-regulated, indicating that **C4** inhibited EMT transformation by regulating the expression of mesenchymal markers and inhibited the invasion and migration of cancer cells.

It is concluded that these SNON donor ligands based Pt(II) complexes have the potential to suppress the growth, invasion, EMT and tumorigenesis of TNBC of which **C4** has the best antitumor activity. **C4** inhibited the cell cycle progression and proliferation of cancer cells by targeting cyclin-dependent kinase CDK4/6 and MYC/STAT3/CCND1/CNNE1 axis. **C4** suppressed the clonogenic potential and spheroids formation ability of TNBC cells, which suggested that **C4** could be a potential anticancer agent to suppress the clone formation ability and cancer stemness of TNBC. **C4** synergized anticancer effect with palbociclib, JQ1 and paclitaxel, thus suggesting an important chemotherapeutic role of **C4** in TNBC. These results showed the potentials of these complexes as anti-TNBC drugs and further provide a base for further exploration in other types of cancers.

4. Materials and methods

4.1. Chemistry

4.1.1. General experimental and materials

All the solvents and reagents involved in the experimental work and test process were purchased from commercial sources. The solvents used in ^{1}H and ^{13}C NMR spectroscopy were DMSO-d_6/D_2O and the test instrument was Bruker AVANCE II 500 MHz machine. HR-ESI-MS spectra of **C1-C6** were measured using water G2-Xs QTof mass spectrometer using a CH_2Cl_2 solution of each complex. Crystal data for **C1**, **C3**, **C4** and **C6** were collected at rt or low temperature on a Rigaku Oxford Diffraction Supernova Dual Source, Cu at Zero equipped with an AtlasS2 CCD using Cu Kα radiation. Oxford Diffraction, Xcalibur CCD System. CrysAlisPro. is used for data acquisition. Oxford Diffraction Ltd: Abingdon, England, UK, 201024. The structures were solved by direct methods using Olex2 software [109] and the non-hydrogen atoms were located from the trial structure and then refined anisotropically with SHELXL-2018 [110] using a full-matrix least squares procedure based on F^2. The weighted R factor, wR and goodness-of-fit S values were obtained based on F^2. The hydrogen atom positions were fixed geometrically at the calculated distances and allowed to ride on their parent atoms. Crystallographic data

was submitted to Cambridge Crystallographic Data Center under CCDC 2342977-2342980 for each **C1**, **C3**, **C4** and **C6**. All this data can be obtained by email at: deposit@ccdc.cam.ac.uk, tel: +44-1223336408 and fax: +44-1223336003.

*4.1.2. General procedure for the synthesis of **C1–C6***

0.1 mmol of the particular starting complex (**SC1-SC6**) [63, 65] and 1.2 equivalents 1.2 mmol of $AgBF_4$ were taken 20 mL of 40% methanol/CH_2Cl_2 solvent mixture and stirred vigorously at reflux (50 °C). After 12 h when all the starting complex was consumed (checked by TLC, eluted with 2% methanol/CH_2Cl_2 mixture), the reaction mixture was cooled to rt and further diluted to 50 mL with 40% methanol/CH_2Cl_2 mixture. It was filtered through celite to remove the black solid that was further washed with 40% methanol/CH_2Cl_2 mixture. The filtrate was added with excess 2 mL of ammonium hydroxide and further stirred at rt till completion (checked by TLC, eluted with 2% methanol/CH_2Cl_2 mixture). After 6 h when all the starting materials were consumed and a single spot of the product was observed on the TLC plate the reaction mixture was evaporated to dryness. 10 mL of deionized water was added and stirred for a while that precipitated a yellow to orange solid, the solid was filtered and washed with deionized water and dried in air to stable mass. Each complex was obtained in good yield and was further characterized in detail.

C1, 72% yield, light yellow solid. FT-IR (KBr pellet) cm^{-1}: 3445, 2926, 1641, 1399, 1066, 672, 543. ^{1}H NMR (500 MHz, DMSO-d_6) δ 9.60 (s, 1H), 8.46 (d, J = 8.6 Hz, 1H), 8.12 (dd, J = 7.9, 1.5 Hz, 1H), 7.94 (dd, J = 8.1, 1.8 Hz, 1H), 7.69-7.62 (m, 2H), 7.53 (t, J = 7.5 Hz, 1H), 7.08 (d, J = 8.6 Hz, 1H), 6.87 (t, J = 7.5 Hz, 1H), 5.01 (s, 3H), 2.99 (s, 3H). ^{13}C NMR (125 MHz, DMSO-d_6) δ 162.22, 155.18, 152.17, 137.63, 136.95, 132.26, 132.15, 130.08, 128.70, 121.39, 120.53, 119.02, 117.96, 28.83ppm. HRMS (ESI): Calcd for $C_{14}H_{15}N_2OPtS$, 454.0553: Found: 454.0553, $[M\text{-}BF_4]^+$.

C2, 78% yield, light yellow solid. FT-IR (KBr pellet) cm^{-1}: 3439, 2921, 1641, 1533, 1399, 1049, 668,551. ^{1}H NMR (500 MHz, DMSO-d_6) δ 9.57 (s, 1H), 8.47 (d, J = 8.6 Hz, 1H), 8.14 (d, J = 7.8 Hz, 1H), 7.73 (s, 1H), 7.63 (t, J = 7.7 Hz, 1H), 7.52 (t, J = 8.0 Hz, 3H), 7.00 (d, J = 8.7 Hz, 1H), 5.01 (s, 3H), 3.00 (s, 3H), 2.30 (s, 3H). ^{13}C NMR (125 MHz, DMSO-d_6) δ 160.72, 154.71, 152.22, 139.34, 135.47, 132.26, 132.14, 129.91, 128.64, 126.26, 120.91, 120.33, 118.88, 28.79, 20.08ppm. HRMS (ESI): Calcd for $C_{15}H_{17}N_2OPtS$, 468.0709: Found: 468.0704, $[M\text{-}BF_4]^+$.

C3, 81% yield, light yellow solid. FT-IR (KBr pellet) cm^{-1}: 3453, 2921, 1637, 1079, 668, 538. ^{1}H NMR (500 MHz, DMSO-d_6) δ 9.61 (s, 1H), 8.41 (d, J = 8.4 Hz, 1H), 8.15 (d, J = 7.7 Hz, 1H), 7.76 (d, J = 9.5 Hz, 1H), 7.65 (t, J = 7.6 Hz, 1H), 7.56 (dt, J = 15.2, 7.1 Hz, 2H), 7.06 (dd, J = 9.0, 4.3 Hz, 1H), 5.04 (s,

3H), 3.00 (s, 3H). ^{13}C NMR (125 MHz, DMSO-d_6) δ 159.03, 154.82, 154.47, 152.96, 151.95, 132.31, 132.19, 130.32, 128.93, 126.15, 125.95, 122.14, 122.07, 120.34, 120.27, 119.09, 118.99, 118.91, 28.80ppm. HRMS (ESI): Calcd for $C_{14}H_{14}FN_2OPtS$, 472.0459: Found: 472.0457, $[M\text{-}BF_4]^+$.

C4, 79% yield, light yellow solid. FT-IR (KBr pellet) cm^{-1}: 3444, 2930, 1641, 1040, 668, 543. ^{1}H NMR (500 MHz, DMSO-d_6) δ 9.69 (s, 1H), 8.55 (d, J = 8.5 Hz, 1H), 7.99 (dd, J = 8.2, 1.8 Hz, 1H), 7.89 (dd, J = 7.9, 1.4 Hz, 1H), 7.87-7.80 (m, 2H), 7.71-7.63 (m, 2H), 7.56-7.44 (m, 4H), 7.08 (d, J = 8.6 Hz, 1H), 6.91 (t, J = 7.4 Hz, 1H), 4.99 (s, 3H). ^{13}C NMR (125 MHz, DMSO-d_6) δ 162.28, 155.67, 152.12, 137.83, 137.07, 132.85, 132.62, 132.19, 132.09, 131.97, 130.58, 130.53, 128.87, 121.41, 120.40, 119.26, 118.15ppm. HRMS (ESI): Calcd for $C_{19}H_{17}N_2OPtS$, 516.0709: Found: 516.0708, $[M\text{-}BF_4]^+$.

C5, 88% yield, light yellow solid. FT-IR (KBr pellet) cm^{-1}: 3448, 2926, 1641, 1394, 1312, 1040, 672, 547.^{1}H NMR (500 MHz, DMSO-d_6) δ 9.61 (s, 1H), 8.52 (d, J = 8.6 Hz, 1H), 7.85 (dd, J = 20.1, 7.7 Hz, 3H), 7.76 (s, 1H), 7.63 (t, J = 7.9 Hz, 1H), 7.56-7.48 (m, 4H), 7.44 (t, J = 7.5 Hz, 1H), 7.00 (d, J = 8.7 Hz, 1H), 4.97 (s, 3H), 2.32 (s, 3H). ^{13}C NMR (125 MHz, DMSO-d_6) δ 160.77, 155.24, 152.17, 139.53, 135.59, 132.85, 132.62, 132.14, 132.11, 131.93, 130.57, 130.38, 128.79, 126.50, 120.92, 120.21, 119.11, 20.07 ppm. HRMS (ESI): Calcd for $C_{20}H_{19}N_2OPtS$, 530.0866: Found: 530.0863, $[M\text{-}BF_4]^+$.

C6, 86% yield, light yellow solid. FT-IR (KBr pellet) cm^{-1}: 3444, 2926, 1641, 1074, 672, 534. ^{1}H NMR (500 MHz, DMSO-d_6) δ 9.68 (s, 1H), 8.51 (d, J = 8.6 Hz, 1H), 7.91-7.80 (m, 3H), 7.64 (t, J = 7.4 Hz, 1H), 7.57-7.37 (m, 6H), 7.03 (d, J = 9.3 Hz, 1H), 4.97 (s, 3H), 3.80 (s, 3H). ^{13}C NMR (125 MHz, DMSO-d_6) δ 158.13, 154.82, 152.25, 150.96, 132.92, 132.62, 132.17,132.12, 131.95, 130.59, 130.35, 128.83, 128.69, 121.44, 120.24, 119.00, 115.12, 56.07ppm. HRMS (ESI): Calcd for $C_{20}H_{19}N_2O_2PtS$, 546.0815: Found: 546.0812, $[M\text{-}BF_4]^+$.

4.2. Biology

4.2.1. Cell culturing

MDA-MB-231, MDA-MB-468 and MDA-MB-436 triple-negative breast cancer cells were obtained from ATCC and maintained in DMEM (Gibco) supplemented with 10% FBS (Gibco) and 1% PEST (penicillin-streptomycin) (Merk Millipore). Cells were grown in 37 ℃ and 5% CO_2 incubator.

4.2.2. Cell viability assay

Cell viability assay was performed using MTT assay. MDA-MB-231, MDA-MB-468 and MDA-MB-436 cells were plated in 96 well plates and next day treated with indicated concentartion of **C1-C6** for 48 h followed by MTT assay. MTT reagent (3-(4,5-Dimethylthiazol-2-yl)-2,5-Diphenyltetrazolium Bromide) (Thermo Fisher Scientific) was added to each 96 well for 2 h and 96 well plates were incubated at 37 ℃ in 5% CO_2 incubator. After 2 h media conataining MTT was removed and then 100 µL of DMSO was added to each well to dissolve formazan crystals. Readings wre taken at 490 nm and data analysis was performed.

4.2.3. Clonogenic assay

MDA-MB-231, MDA-MB-468 and MDA-MB-436 cells were seedeed in 24 well plates and then next day treated with DMSO, 2.5 and 5 µM of **C4**. After 3 days treatment, old media was removed from plates and fresh media was added. After total 7 days of incubation, media was removed from cells and washed 3 times with 1XPBS. Cells were then fixed with (acetic acid:methanol 1: 7) fixation solution for 20 min at rt. After removal of fixation solution, cells were stained with 0.5% crystal violet (Sigma Aldrich) solution for 20 min at rt. After removal of crystal violet solution, cells were washed with tap water 3-5 times to remove excess crystal violet dye. Plates were dried and then scanned to take images. After that a mixture of 50% ethanol and acetic acid (1: 1) solution was added to each well and readings were performed at 570 nm.

4.2.4. Invasion assay

For invasion assay MDA-MB-231, MDA-MB-468 and MDA-MB-436 cells were plated into transwell inserts (Corning, USA). Transwell inserts were pre-coated with matrigel (BD). MDA-MB-231, MDA-MB-468 and MDA-MB-436 cells were treated with DMSO and **C4**. Lower part of chambers were filled with 500 µL medium supplemented with 20% FBS. After 24 h of incubation, cells those penetrated were fixed with fixation solution (methanol) for 20 min at rt. After that cells were stained with 0.5% crystal violet solution for 20 min at rt. Chambers were washed with water to remove excess of crystal violet solution and images were taken.

4.2.5. Mammosphere/spheroids formation assay

MDA-MB-231, MDA-MB-468 and MDA-MB-436 cells were grown as mammosphere/ spheroids in 96 well ultra-low attachment plates (Corning) and then treated with DMSO or **C4** (5 µM) for 7 days. Mammosphere/spheroids medium was prepared using B27 supplement (Thermo Fisher Scientific), DMEM / F12 medium (Thermo Fisher Scientific), basic fibroblast growth factor (bFGF) (Sigma Aldrich)

and epidermal growth factor (EGF) (Thermo Fisher Scientific). After 7 days of incubation bright field images were taken.

4.2.6. Drugs synergism study

MDA-MB-231, MDA-MB-468 and MDA-MB-436 cells were plated in 96 well plates and then treated with **C4**, JQ1, Palbociclib, and Paclitaxel alone or in combination (**C4** and JQ1 combination), (**C4** and Palbociclib combination) and (**C4** and Paclitaxel combination) and then MTT assay was performed to determine cell proliferation. For synergism study, drug combination index (CI) was calculated according to the method described by Chou–Talalay [111]. CI < 1 synergism, CI = 1 additive effect and CI > 1 antagonism. Statistical analysis was performed using unpaired student t test. $P<0.05$*, $P < 0.005$** was considered statistically significant.

4.2.7. RNA extarction and RT-PCR

MDA-MB-231, MDA-MB-468 and MDA-MB-436 breast cancer cells were plated in 96 well plates, next day treated with DMSO or **C4** for 48 h. TRIzol reagent (Invitrogen, USA) was used to extract the total RNA following the protocol. PrimeScript TM RT Reagent Kit (Takara, Japan) was used for reverse transcription. After that RT-PCR analysis was performed using SYBR Green Master Mix following the instructions from manufacturer. β-actin was used as internal control. Following primers were used;

MYC:

Forward Sequence	CCTGGTGCTCCATGAGGAGAC
Reverse Sequence	CAGACTCTGACCTTTTGCCAGG

STAT3:

Forward Sequence	CTTTGAGACCGAGGTGTATCACC
Reverse Sequence	GGTCAGCATGTTGTACCACAGG

CCND1:

Forward Sequence	TCTACACCGACAACTCCATCCG
Reverse Sequence	TCTGGCATTTTGGAGAGGAAGTG

CCND1:	
Forward Sequence	TGTGTCCTGGATGTTGACTGCC
Reverse Sequence	CTCTATGTCGCACCACTGATACC
P27:	
Forward Sequence	ATAAGGAAGCGACCTGCAACCG
Reverse Sequence	TTCTTGGGCGTCTGCTCCACAG
TWIST1:	
Forward Sequence	GCCAGGTACATCGACTTCCTCT
Reverse Sequence	TCCATCCTCCAGACCGAGAAGG
SLUG:	
Forward Sequence	ATCTGCGGCAAGGCGTTTTCCA
Reverse Sequence	GAGCCCTCAGATTTGACCTGTC
ZEB1:	
Forward Sequence	GGCATACACCTACTCAACTACGG
Reverse Sequence	TGGGCGGTGTAGAATCAGAGTC
Vimentin:	
Forward Sequence	AGGCAAAGCAGGAGTCCACTGA
Reverse Sequence	ATCTGGCGTTCCAGGGACTCAT
ZO-1	
Forward Sequence	GTCCAGAATCTCGGAAAAGTGCC
Reverse Sequence	CTTTCAGCGCACCATACCAACC

4.2.8. Western blot

MDA-MB-231, MDA-MB-468 and MDA-MB-436 cells were plated in 96 well plates, next day treated with DMSO or **C4**. After treatment for 48 h, cells were collected as a pellet. Then cell pellets were washed with 1XPBS and RIPA lysis buffer containing 1.0% NP-40, 50 μM Tris (pH 8.0), 120 μM sodium chloride 0.1% SDS and 0.5% sodium deoxycholate along with protease inhibitors cocktail. Lysis was perfromed for 30 minutes on ice and then centrifugation was performed at 4 ℃ for 15 min and supernatant was collected. Protein quantification was performed and then samples were boiled at 95 ℃ for 5 min in 5X loading buffer. Samples were run on gel and PVDF membrane was used for transfer process. Blocking was performed using 5% non-fat dry milk that in 1X TBST. For 1 h at rt. Then membranes were incubated with indicated primary antibodies for overnight at 4 ℃. Next day, primary antibodies were removed and then membrane was washed with 1X TBST for three times. Membranes were then incubated with secondary antibody for 2 h at rt. Then secondary antibody was removed from membrane and washed with 1X TBST three times. ECL solution (Pierce™ ECL Western Blotting Substrate) was used to detect the signal. CDK4 (D9G3E) Rabbit mAb #12790 (cell signaling technology), CDK6 (D4S8S) Rabbit mAb #13331(cell signaling technology) and α-Tubulin Antibody #2144 (cell signaling technology).

Acknowledgements

The authors acknowledge the Inner Mongolia University China funding under the title Academic Backbone (No. 10000-21311201/092), Inner Mongolia Autonomous Region China Funding No. 21300-5213122 and "JUN-MA" High-level Talents Program of Inner Mongolia University China (No. 21300-5195112, No. 21300-5205107).

Appendix A. Supplementary data

Supplementary data, stability figures, ^{1}H, ^{13}C, and MS spectra and other related data to this article can be found at http://dx.doi.org/10.

References

[1] Y. Li, H. Zhang, Y. Merkher, L. Chen, N. Liu, S. Leonov and Y. Chen, Recent advances in therapeutic strategies for triple-negative breast cancer, Journal of Hematology & Oncology, 15 (2022) 121.

[2] J. G. P. Pandy, J. C. B. Garcia, M. V. B. C. Ordinario and F. V. F. Que, Triple negative breast cancer and platinum-based systemic treatment: a meta-analysis and systematic review, BMC Cancer, 19 (2019) 1065.

[3] Y. Shi, J. Jin, W. Ji and X. Guan, Therapeutic landscape in mutational triple negative breast cancer, Molecular Cancer, 17 (2018) 99.

[4] K. Asleh, N. Riaz and T. O. Nielsen, Heterogeneity of triple negative breast cancer: Current advances in subtyping and treatment implications, Journal of Experimental & Clinical Cancer Research, 41 (2022) 265.

[5] L. Yin, J. J. Duan, X. W. Bian and S. C. Yu, Triple-negative breast cancer molecular subtyping and treatment progress, Breast Cancer Research, 22 (2020) 61.

[6] A. C. Watt and S. Goel, Cellular mechanisms underlying response and resistance to CDK4/6 inhibitors in the treatment of hormone receptor-positive breast cancer, Breast Cancer Research, 24 (2022) 17.

[7] Y. Yang, J. Luo, X. Chen, Z. Yang, X. Mei, J. Ma, Z. Zhang, X. Guo and X. Yu, CDK4/6 inhibitors: a novel strategy for tumor radiosensitization, Journal of Experimental & Clinical Cancer Research, 39 (2020) 188.

[8] M. A. George, S. Qureshi, C. Omene, D. L. Toppmeyer and S. Ganesan, Clinical and pharmacologic differences of CDK4/6 inhibitors in breast cancer, Frontiers in Oncology, 11 (2021) 693104.

[9] Q. Du, X. Guo, M. Wang, Y. Li, X. Sun and Q. Li, The application and prospect of CDK4/6 inhibitors in malignant solid tumors, Journal of Hematology & Oncology, 13 (2020) 41.

[10] H. Xu, S. Yu, Q. Liu, X. Yuan, S. Mani, R. G. Pestell and K. Wu, Recent advances of highly selective CDK4/6 inhibitors in breast cancer, Journal of Hematology & Oncology, 10 (2017) 97.

[11] S. Alassadi, M. J. Pisani and N. J. Wheate, A chemical perspective on the clinical use of platinum-based anticancer drugs, Dalton Transactions, 51 (2022) 10835 - 10846.

[12] B. Lippert and P. J. Sanz Miguel, More of a misunderstanding than a real mismatch? Platinum and its affinity for aqua, hydroxido, and oxido ligands, Coordination Chemistry Reviews, 327-328 (2016) 333 - 348.

[13]]A. K. Gorle, S. J. B. Price and N. P. Farrell, Biological relevance of interaction of platinum drugs with O-donor ligands, Inorganica Chimica Acta, 495 (2019) 118974.

[14] T. Tippayamontri, R. Kotb, B. Paquette and L. Sanche, Cellular uptake and cytoplasm / DNA distribution of cisplatin and oxaliplatin and their liposomal formulation in human colorectal cancer cell HCT116, Invest New Drugs, 29 (2011) 1321 - 1327.

[15] M. Groessl, O. Zava and P. J. Dyson, Cellular uptake and subcellular distribution of ruthenium-based metallodrugs under clinical investigation versus cisplatin, Metallomics, 3 (2011) 591 - 599.

[16] T. C. Johnstone, J. J. Wilson and S. J. Lippard, Monofunctional and higher-valent platinum anticancer agents, Inorganic Chemistry, 52 (2013) 12234 - 12249.

[17] W. P. McGuire and M. Markman, Primary ovarian cancer chemotherapy: current standards of care, British Journal of Cancer, 89 (2003) S3 - 8.

[18] V. Brabec, O. Hrabina and J. Kasparkova, Cytotoxic platinum coordination compounds. DNA binding agents, Coordination Chemistry Reviews, 351 (2017) 2 - 31.

[19] B. Koberle, M. T. Tomicic, S. Usanova and B. Kaina, Cisplatin resistance: preclinical findings and clinical implications, Biochimica et Biophysica Acta, 1806 (2010) 172 - 182.

[20] P. Lv, S. Man, L. Xie, L. Ma and W. Gao, Pathogenesis and therapeutic strategy in platinum resistance lung cancer, Biochimica et Biophysica Acta (BBA) - Reviews on Cancer, 1876 (2021) 188577.

[21] N. Cutillas, G. S. Yellol, C. de Haro, C. Vicente, V. Rodríguez and J. Ruiz, Anticancer cyclometalated complexes of platinum group metals and gold, Coordination Chemistry Reviews, 257 (2013) 2784 - 2797.

[22] T. R. Panda, M. M, S. P. Vaidya, S. Chhatar, S. Sinha, M. Mehrotra, S. Chakraborty, S. Gadre, P. Duari, P. Ray and M. Patra, The Power of Kinetic Inertness in Improving Platinum Anticancer Therapy by Circumventing Resistance and Ameliorating Nephrotoxicity, Angewandte Chemie International Edition, 62 (2023) e202303958.

[23] J. L. M. Digby, T. Vanichapol, A. Przepiorski, A. J. Davidson and X. V. Sander, Evaluation of cisplatin-induced injury in human kidney organoids, American Journal of Physiology-Renal Physiology, 318 (2020) F971 - F978.

[24] T. Zhong, J. Yu, Y. Pan, N. Zhang, Y. Qi and Y. Huang, Recent advances of platinum-based anticancer complexes in combinational multimodal therapy, Advanced Healthcare Materials, 12 (2023) e2300253.

[25] G. Coffetti, M. Moraschi, G. Facchetti and I. Rimoldi, The challenging treatment of cisplatin-resistant tumors: state of the art and future perspectives, Molecules, 28 (2023) 3407.

[26] Y. Zhu, Y. Hu, C. Tang, X. Guan and W. Zhang, Platinum-based systematic therapy in triple-negative breast cancer, Biochimica et Biophysica Acta (BBA) - Reviews on Cancer, 1877 (2022) 188678.

[27] A. C. Famurewa, A. G. Mukherjee, U. R. Wanjari, A. Sukumar, R. Murali, K. Renu, B. Vellingiri, A. Dey and A. V. Gopalakrishnan, Repurposing FDA-approved drugs against the toxicity of platinum-based anticancer drugs, Life Sciences, 305 (2022) 120789.

[28] U. Basu, B. Banik, R. Wen, R. K. Pathak and S. Dhar, The Platin-X series: activation, targeting, and delivery, Dalton Transactions, 45 (2016) 12992 - 13004.

[29] H. Nasu, S. Nishio, J. Park, T. Yoshimitsu, K. Matsukuma, K. Tasaki, T. Katsuda, A. Terada, N. Tsuda and K. Ushijima, Platinum rechallenge treatment using gemcitabine plus carboplatin with or without bevacizumab for platinum-resistant ovarian cancer, International Journal of Clinical Oncology, 27 (2022) 790 - 801.

[30] B. W. Harper, A. M. K. Heuer, M. P. Grant, M. Manohar, K. B. G. Singh and J. R. A. Wright, Advances in platinum chemotherapeutics, Chemistry, 16 (2010) 7064 - 7077.

[31] I. S. Song, N. Savaraj, Z. H.Siddik, P. Liu, Y. Wei, C. J. Wu and M. T. Kuo, Role of human copper transporter Ctr1 in the transport of platinum-based antitumor agents in cisplatin-sensitive and cisplatin-resistant cells, Molecular Cancer Therapeutics, 3 (2004) 1543 -1549.

[32] G. Ferraro, V. Sanfilippo, L. Chiaverini, C. Satriano, T. Marzo, A. Merlino and D. La Mendola, Cisplatin binding to angiogenin protein: new molecular pathways and targets for the drug's anticancer activity, Dalton Transactions, 52 (2023) 9058 - 9067.

[33] S. J. B. Price, Activating platinum anticancer complexes with visible light, Angewandte Chemie International Edition, 50 (2011) 804 - 805.

[34] L. Ma, N. Wang, R. Ma, C. Li, Z. Xu, M. K. Tse and G. Zhu, Monochalcoplatin: An Actively Transported, Quickly Reducible, and Highly Potent Pt(IV) Anticancer Prodrug, Angewandte Chemie International Edition, 57 (2018) 9098 - 9102.

[35] P. Liu, Y. Lu, X. Gao, R. Liu, D. Z. Negrerie, Y. Shi, Y. Wang, S. Wang and Q. Gao, Highly water-soluble platinum(II) complexes as GLUT substrates for targeted therapy: improved anticancer efficacy and transporter-mediated cytotoxic properties, Chemical Communications, 49 (2013) 2421 - 2423.

[36] L. Quan, Z. Lin, Y. Lin, Y. Wei, L. Lei, Y. Li, G. Tan, M. Xiao and T. Wu, Glucose-modification of cisplatin to facilitate cellular uptake, mitigate toxicity to normal cells, and improve anti-cancer effect in cancer cells, Journal of Molecular Structure, 1203 (2020) 127361.

[37] M. Ravera, E. Gabano, M. J. Mcglinchey and D. Osella, A view on multi-action Pt(IV) antitumor prodrugs, Inorganica Chimica Acta, 492 (2019) 32 - 47.

[38] S. Su, Y. Chen, P. Zhang, R. Ma, W. Zhang, J. Liu, T. Li, H. Niu, Y. Cao, B. Hu, J. Gao, H. Sun, D. Fang, J. Wang, P. G. Wang, S. Xie, C. Wang and J. Ma, The role of Platinum(IV)-based antitumor drugs and the anticancer immune response in medicinal inorganic chemistry. A systematic review from 2017 to 2022, European Journal of Medicinal Chemistry, 243 (2022) 114680.

[39] S. Jin, Y. Guo, Z. Guo and X. Wang, Monofunctional platinum(II) anticancer agents, Pharmaceuticals, 14 (2021) 133.

[40] D. A. Arantseva and E. L. Vodovozova, Platinum-based antitumor drugs and their liposomal formulations in clinical trials, Russian Journal of Bioorganic Chemistry, 44 (2019) 619 - 630.

[41] Z. Y. Ma, D. B. Wang, X. Q. Song, Y. G. Wu, Q. Chen, C. L. Zhao, J. Y. Li, S. H. Cheng and J. Y. Xu, Chlorambucil-conjugated platinum(IV) prodrugs to treat triple-negative breast cancer *in vitro* and *in vivo*, European Journal of Medicinal Chemistry, 157 (2018) 1292 - 1299.

[42] K. M. Deo, J. Sakoff, J. Gilbert, Y. Zhang and J. R. Aldrich Wright, Synthesis, characterisation and influence of lipophilicity on cellular accumulation and cytotoxicity of unconventional platinum(iv) prodrugs as potent anticancer agents, Dalton Transactions, 48 (2019) 17228 - 17240.

[43] M.Coluccia and G. Natile, Trans-platinum complexes in cancer therapy, Anti-Cancer Agents in Medicinal Chemistry, 7 (2007) 111 - 123.

[44] S. M. Aris, D. A. Gewirtz, J. J. Ryan, K. M. Knott and N. P. Farrell, Promotion of DNA strand breaks, interstrand cross-links and apoptotic cell death in A2780 human ovarian cancer cells by transplatinum planar amine complexes, Biochemical Pharmacology, 73 (2007) 1749 - 1757.

[45] U. K. Lis, J. Ochocki and K. M. Wasowska, Trans geometry in platinum antitumor complexes, Coordination Chemistry Reviews, 252 (2008) 1328 - 1345.

[46] S. M. Aris and N. P. Farrell, Towards antitumor active trans-platinum compounds, European Journal of Inorganic Chemistry, 2009 (2009) 1293.

[47] C. Musetti, A. A. Nazarov, N. P. Farrell and C. Sissi, DNA reactivity profile of trans-platinum planar amine derivatives, ChemMedChem, 6 (2011) 1283 - 1290.

[48] X. He, J. Yu, R. Yin, P. Zhang, C. Xiao and X. Chen, A Nanoscale Trans-Platinum(II)-Based Supramolecular Coordination Self-Assembly with a Distinct Anticancer Mechanism, Advanced Materials, (2024) 2312488.

[49] C. Icsel, V. T. Yilmaz, F. Ari, E. Ulukaya and W. T. Harrison, trans-Dichloridopalladium(II) and platinum(II) complexes with 2-(hydroxymethyl)pyridine and 2-(2-hydroxyethyl)pyridine:

synthesis, structural characterization, DNA binding and *in vitro* cytotoxicity studies, European Journal of Medicinal Chemistry, 60 (2013) 386 - 394.

[50] N. Aztopal, D. Karakas, B. Cevatemre, F. Ari, C. Icsel, M. G. Daidone and E. Ulukaya, A trans-platinum(II) complex induces apoptosis in cancer stem cells of breast cancer, Bioorganic & Medicinal Chemistry, 25 (2017) 269 - 276.

[51] G. C. Fortman and S. P. Nolan, N-Heterocyclic carbene (NHC) ligands and palladium in homogeneous cross-coupling catalysis: a perfect union, Chemical Society Reviews, 40 (2011) 5151 - 5169.

[52] A. K. Nebioglu, M. J. Panzner, C. A. Tessier, C. L. Cannon and W. J. Youngs, N-heterocyclic carbene-silver complexes: a new class of antibiotics, Coordination Chemistry Reviews, 251 (2007) 884 - 895.

[53] A. John and P. Ghosh, Fascinating frontiers of N/O-functionalized N-heterocyclic carbene chemistry: from chemical catalysis to biomedical applications, Dalton Transactions, 39 (2010) 7183 - 7206.

[54] E. Chardon, G. L. Puleo, G. Dahm, G. Guichard and S. Bellemin-Laponnaz, Direct functionalisation of group 10 N-heterocyclic carbene complexes for diversity enhancement, Chemical Communications, 47 (2011) 5864 - 5866.

[55] M. Skander, P. Retailleau, B. Bourrie, L. Schio, P. Mailliet and A. Marinetti, N-heterocyclic carbene-amine Pt(II) complexes, a new chemical space for the development of platinum-based anticancer drugs, Journal of Medicinal Chemistry, 53 (2010) 2146 - 2154.

[56] M. Chtchigrovsky, L. Eloy, H. Jullien, L. Saker, E. S. Bendirdjian, J. Poupon, S. Bombard, T. Cresteil, P. Retailleau and A. Marinetti, Antitumor trans-N-heterocyclic carbene-amine-Pt(II) complexes: synthesis of dinuclear species and exploratory investigations of DNA binding and cytotoxicity mechanisms, Journal of Medicinal Chemistry, 56 (2013) 2074 - 2086.

[57] T. Jia, O. Diane, D. Ghosh, M. Skander, G. Fontaine, P. Retailleau, J. Poupon, J. Bignon, Y. M. M. Siasia, V. Servajean, N. Hue, J. F. Betzer, A. Marinetti and S. Bombard, Anti-cancer and radio-sensitizing properties of new bimetallic (N-heterocyclic carbene)-amine-Pt(II) complexes, Journal of Medicinal Chemistry, 66 (2023) 6836 - 6848.

[58] F. J. R. Lima, A. G. Quiroga, B. G. Serrelde, F. Blanco, A. Carnero and C. N. Ranninger, New trans-platinum drugs with phosphines and amines as carrier ligands induce apoptosis in tumor cells resistant to cisplatin, Journal of Medicinal Chemistry, 50 (2007) 2194 - 2199.

[59] M. Kumar, A. K. Singh, V. K. Singh, R. K. Yadav, A. P. Singh and S. Singh, Recent developments in the biological activities of 3d-metal complexes with salicylaldehyde-based N, O-donor schiff base ligands, Coordination Chemistry Reviews, 505 (2024) 215663.

[60] X. G. Bai, Y. Zheng and J. Qi, Advances in thiosemicarbazone metal complexes as antilung cancer agents, Frontiers in Pharmacology, 13 (2022) 1018951.
[61] A. I. Matesanz, J. M. Herrero, E. J. Faraco, L. Cubo and A. G. Quiroga, New patinum(II) triazole thiosemicarbazone complexes: analysis of their reactivity and potential antitumoral action, Chemical biology chemistry, 21 (2020) 1226 - 1232.
[62] A. I. Matesanz, E. J. Faraco, M. C. Ruiz, L. M. Balsa, C. Navarro-Ranninger, I. E. León and A. G. Quiroga, Mononuclear Pd(ii) and Pt(ii) complexes with an α-N-heterocyclic thiosemicarbazone: cytotoxicity, solution behaviour and interaction versus proven models from biological media, Inorganic Chemistry Frontiers, 5 (2018) 73 - 83.
[63] X. Bai, A. Ali, Z. Lv, N. Wang, X. Zhao, H. Hao, Y. Zhang and F. U. Rahman, Platinum complexes inhibit HER-2 enriched and triple-negative breast cancer cells metabolism to suppress growth, stemness and migration by targeting PKM/LDHA and CCND1/BCL2/ATG3 signaling pathways, European Journal of Medicinal Chemistry, 224 (2021) 113689.
[64] X. Bai, A. Ali, N. Wang, Z. Liu, Z. Lv, Z. Zhang, X. Zhao, H. Hao, Y. Zhang and F. U. Rahman, Inhibition of SREBP-mediated lipid biosynthesis and activation of multiple anticancer mechanisms by platinum complexes: ascribe possibilities of new antitumor strategies, European Journal of Medicinal Chemistry, 227 (2022) 113920.
[65] F. U. Rahman, A. Ali, H. Q. Duong, I. U. Khan, M. Z. Bhatti, Z. T. Li, H. Wang and D. W. Zhang, ONS-donor ligand based Pt(II) complexes display extremely high anticancer potency through autophagic cell death pathway, European Journal of Medicinal Chemistry, 164 (2019) 546 - 561.
[66] N. Wang, A. Ali, Z. Liu, H. Chi, Z. Lv, X. Zhao, Z. Zhang, H. Hao, Y. Zhang and F. U. Rahman, Monofunctional dimetallic Ru(eta6-arene) complexes inhibit NOTCH1 signaling pathway and synergistically enhance anticancer effect in combination with cisplatin or vitamin C, European Journal of Medicinal Chemistry, 258 (2023) 115536.
[67] S. Ahmad, Kinetic aspects of platinum anticancer agents, Polyhedron, 138 (2017) 109 - 124.
[68] M. D. Hall, K. A. Telma, K. E. Chang, T. D. Lee, J. P. Madigan, J. R. Lloyd, I. S. Goldlust, J. D. Hoeschele and M. M. Gottesman, Say no to DMSO: dimethylsulfoxide inactivates cisplatin, carboplatin, and other platinum complexes, Cancer Research, 74 (2014) 3913 - 3922.
[69] J. Reedijk, Platinum anticancer coordination compounds: study of DNA binding inspires new drug design, European Journal of Inorganic Chemistry, 2009 (2009) 1303 - 1312.
[70] J. A. Young, A. R. Tan, Targeted treatment of triple-negative breast cancer, The Cancer Journal, 27 (2021) 50 - 58.

[71] M. Pont, M. Marques, M. A. Sorolla, E. Parisi, I. Urdanibia, S. Morales, A. Salud and A. Sorolla, Applications of CRISPR technology to breast cancer and triple negative breast cancer research, Cancers, 15 (2023) 4364.
[72] S. Kunou, K. Shimada, T. Hikita, T. Aoki, A. Sakamoto, F. Hayakawa, C. Oneyama and H. Kiyoi, Exosomes derived from cancer associated fibroblasts elicit survival and drug resistance of primary lymphoma cells, Blood, 132 (2018) 4128.
[73] L. Jin, J. Chun, C. Pan, G. N. Alesi, D. Li, K. R. Magliocca, Y. Kang, Z. G. Chen, D. M. Shin, F. R. Khuri, J. Fan and S. Kang, Phosphorylation-mediated activation of LDHA promotes cancer cell invasion and tumour metastasis, Oncogene, 36 (2017) 3797 - 3806.
[74] A. Banerjee, D. Deka, M. Muralikumar, A. S. Zhang, A. Bisgin, C. Christopher, H. Zhang, X. F. Sun and S. Pathak, A concise review on miRNAs as regulators of colon cancer stem cells and associated signalling pathways, Clinical and Translational Oncology, 25 (2023) 3345 - 3356.
[75] X. Wang, W. Shi, X. Wang, J. J. Lu, P. He, H. Zhang and X. Chen, Nifuroxazide boosts the anticancer efficacy of palbociclib-induced senescence by dual inhibition of STAT3 and CDK2 in triple-negative breast cancer, Cell Death Discovery, 9 (2023) 355.
[76] J. Y. Ge, S. Shu, M. Kwon, B. Jovanovic, K. Murphy, A. Gulvady, A. Fassl, A. Trinh, Y. Kuang, G. A. Heavey, A. Luoma, C. Paweletz, A. R. Thorner, K. W. Wucherpfennig, J. Qi, M. Brown, P. Sicinski, T. O. McDonald, D. Pellman, F. Michor and K. Polyak, Acquired resistance to combined BET and CDK4/6 inhibition in triple-negative breast cancer, Nature Communications, 11 (2020) 2350.
[77] H. Yuan, H. Guo, X. Luan, M. He, F. Li, J. Burnett, N. Truchan and D. Sun, Albumin Nanoparticle of Paclitaxel (Abraxane) Decreases while Taxol Increases Breast Cancer Stem Cells in Treatment of Triple Negative Breast Cancer, Molecular Pharmaceutics, 17 (2020) 2275 - 2286.
[78] J. H. Ma, L. Qin and X. Li, Role of STAT3 signaling pathway in breast cancer, Cell Communication and Signaling, 18 (2020) 33.
[79] M. J. Duffy, S. O'Grady, M. Tang and J. Crown, MYC as a target for cancer treatment, Cancer Treatment Reviews, 94 (2021) 102154.
[80] M. F. Z. Fluck, L. Soucek and J. R. Whitfield, MYC: there is more to it than cancer, Frontiers in Cell and Developmental Biology, 12 (2024) 1342872.
[81] M. Wanzel, S. Herold and M. Eilers, Transcriptional repression by Myc, Trends in Cell Biology, 13 (2003) 146 - 150.
[82] D. Zimmerli, C. S. Brambillasca, F. Talens, J. Bhin, R. Linstra, L. Romanens, A. Bhattacharya, S. E. P. Joosten, A. M. Da Silva, N. Padrao, M. D. Wellenstein, K. Kersten, M. de Boo, M. Roorda, L. Henneman, R. de Bruijn, S. Annunziato, E. van der Burg, A. P. Drenth, C.

Lutz, T. Endres, M. van de Ven, M. Eilers, L. Wessels, K. E. de Visser, W. Zwart, R. S. N. Fehrmann, M. van Vugt and J. Jonkers, MYC promotes immune-suppression in triple-negative breast cancer via inhibition of interferon signaling, Nature Communications, 13 (2022) 6579.

[83] T. Gharibi, Z. Babaloo, A. Hosseini, M. A. Alitappeh, V. Hashemi, F. Marofi, K. Nejati and B. Baradaran, Targeting STAT3 in cancer and autoimmune diseases, European Journal of Pharmacology, 878 (2020) 173107.

[84] R. G. Kenny and C. J. Marmion, Toward multi-targeted platinum and ruthenium drugs-a new paradigm in cancer drug treatment regimens?, Chemical Reviews, 119 (2019) 1058 - 1137.

[85] F. Guo and J. Xue, MicroRNA‐628‐5p inhibits cell proliferation and induces apoptosis in colorectal cancer through downregulating CCND1 expression levels, Molecular Medicine Reports, 21 (2020) 1481 - 1490.

[86] C. Guarducci, M. Bonechi, M. Benelli, C. Biagioni, G. Boccalini, D. Romagnoli, R. Verardo, R. Schiff, C. K. Osborne, C. D. Angelis, A. D. Leo, L. Malorni and I. Migliaccio, Cyclin E1 and Rb modulation as common events at time of resistance to palbociclib in hormone receptor-positive breast cancer, Nature Partner Journals Breast Cancer, 4 (2018) 38.

[87] L. Chen, X. Miao, C. Si, A. Qin, Y. Zhang, C. Chu, Z. Li, T. Wang and X. Liu, Long non-coding RNA SENP3-EIF4A1 functions as a sponge of miR-195-5p to drive triple-negative breast cancer progress by overexpressing CNNE1, Frontiers in Cell and Developmental Biology, 9 (2021) 647527.

[88] Q. Yuan, L. Zheng, Y. Liao and G. Wu, Overexpression of CNNE1 confers a poorer prognosis in triple-negative breast cancer identified by bioinformatic analysis, World Journal of Surgical Oncology, 19 (2021) 86.

[89] Y. Liu, A. Zhang, P. P. Bao, L. Lin, Y. Wang, H. Wu, X. O. Shu, A. Liu and Q. Cai, MicroRNA-374b inhibits breast cancer progression through regulating CCND1 and TGFA genes, Carcinogenesis, 42 (2021) 528 - 536.

[90] Z. Soleimani, D. Kheirkhah, M. R. Sharif, A. Sharif, M. Karimian and Y. Aftabi, Association of CCND1 gene c.870G>A polymorphism with breast cancer risk: a case-controlStudy and a meta-analysis, Pathology & Oncology Research, 23 (2017) 621 - 631.

[91] M. Ran, H. Luo, H. Gao, X. Tang, Y. Chen, X. Zeng, B. Weng and B. Chen, miR-362 knock-down promotes proliferation and inhibits apoptosis in porcine immature sertoli cells by targeting the RMI1 gene, Reproduction in Domestic Animals, 55 (2020) 547 - 558.

[92] J. Xing, J. Li, L. Fu, J. Gai, J. Guan and Q. Li, SIRT4 enhances the sensitivity of ER-positive breast cancer to tamoxifen by inhibiting the IL-6/STAT3 signal pathway, Cancer Medicine, 8 (2019) 7086 - 7097.

[93] S. F. Razavipour, K. B. Harikumar and J. M. Slingerland, p27 as a Transcriptional regulator: new roles in development and cancer, Cancer Research, 80 (2020) 3451 - 3458.
[94] J. Qi and Z. Ouyang, Targeting CDK4/6 for Anticancer Therapy, Biomedicines, 10 (2022) 685.
[95] R. Wang, K. Xu, F. Gao, J. Huang and X. Guan, Clinical considerations of CDK4/6 inhibitors in triple-negative breast cancer, Biochimica et Biophysica Acta (BBA) - Reviews on Cancer, 1876 (2021) 188590.
[96] Y. Hu, J. Gao, M. Wang and M. Li, Potential prospect of CDK4/6 inhibitors in triple-negative breast cancer, Cancer Management and Research, 13 (2021) 5223 - 5237.
[97] M. A. Fernandez and M. Malumbres, Mechanisms of sensitivity and resistance to CDK4/6 inhibition, Cancer Cell, 37 (2020) 514 - 529.
[98] M. Dai, J. Boudreault, N. Wang, S. Poulet, G. Daliah, G. Yan, A. Moamer, S. A. Burgos, S. Sabri, S. Ali and J. J. Lebrun, Differential regulation of cancer progression by CDK4/6 plays a central role in DNA replication and repair pathways, Cancer Research, 81 (2021) 1332 - 1346.
[99] W. Xue, J. Hao, Q. Zhang, R. Jin, Z. Luo, X. Yang, Y. Liu, Q. Lu, Y. Ouyang and H. Guo, Chlorogenic acid inhibits epithelial-mesenchymal transition and invasion of breast cancer by down-regulating LRP6, Journal of Pharmacology and Experimental Therapeutics, 384 (2023) 254 - 264.
[100] I. G. Soares, D. V. Chartoumpekis, V. Kyriazopoulou and A. Zaravinos, EMT factors and metabolic pathways in cancer, Frontiers in Oncology, 10 (2020) 499.
[101] S. A. M. Imran, M. D. Yazid, R. B. H. Idrus, M. Maarof, A. Nordin, R. A. Razali and Y. Lokanathan, Is there an interconnection between epithelial-mesenchymal transition (EMT) and telomere shortening in aging?, International Journal of Molecular Sciences, 22 (2021) 3888.
[102] S. Usman, N. H. Waseem, T. K. N. Nguyen, S. Mohsin, A. Jamal, M. T. Teh and A. Waseem, Vimentin is at the heart of epithelial mesenchymal transition (EMT) mediated metastasis, Cancers (Basel), 13 (2021) 4985.
[103] M. Wallesch, D. Pachow, C. Blucher, R. Firsching, J. P. Warnke, W. E. K. Braunsdorf, E. Kirches and C. Mawrin, Altered expression of E-Cadherin-related transcription factors indicates partial epithelial-mesenchymal transition in aggressive meningiomas, Journal of the Neurological Sciences, 380 (2017) 112 - 121.
[104] T. Nagai, T. Arao, K. Nishio, K. Matsumoto, S. Hagiwara, T. Sakurai, Y. Minami, H. Ida, K. Ueshima, N. Nishida, K. Sakai, N. Saijo, K. Kudo, H. Kaneda, D. Tamura, K. Aomatsu, H. Kimura, Y. Fujita, S. Haji and M. Kudo, Impact of tight junction protein ZO-1 and TWIST

expression on postoperative survival of patients with hepatocellular carcinoma, Digestive Diseases, 34 (2016) 702 - 707.

[105] H. S. Kim, S. I. Lee, Y. R. Choi, J. Kim, J. W. Eun, K. S. Song and J. Y. Jeong, GNAQ-regulated ZO-1 and ZO-2 act as tumor suppressors by modulating EMT potential and tumor-repressive microenvironment in lung cancer, International Journal of Molecular Sciences, 24 (2023) 8801.

[106] S. Adhikari, P. Nath, A. Das, A. Datta, N. Baildya, A. K. Duttaroy and S. Pathak, A review on metal complexes and its anti-cancer activities: Recent updates from *in vivo* studies, Biomedicine & Pharmacotherapy, 171 (2024) 116211.

[107] R. Lusby, Z. Zhang, A. Mahesh and V. K. Tiwari, Decoding gene regulatory circuitry underlying TNBC chemoresistance reveals biomarkers for therapy response and therapeutic targets, NPJ Precision Oncology , 8 (2024) 64.

[108] X. Dai, H. Cheng, Z. Bai and J. Li, Breast cancer cell line classification and its relevance with breast tumor subtyping, Journal of Cancer, 8 (2017) 3131 - 3141.

[109] O.V. Dolomanov, L.J. Bourhis, R.J. Gildea, J.A.K. Howard, H. Puschmann, OLEX2: a complete structure solution, refinement and analysis program, Archive of Journal of Applied Crystallography, 42 (2009) 339 - 341.

[110] D. Kratzert, J.J. Holstein, I. Krossing, DSR: enhanced modelling and refinement of disordered structures with SHELXL, Archive of Journal of Applied Crystallography, 48 (2015) 933 - 938.

[111] T.-C. Chou Drug Combination Studies and Their Synergy Quantification Using the Chou-Talalay Method, Cancer Res 70 (2) (2010) 440 – 446.